TUNNELING DENSITY OF STATES BEHAVIOR IN SUPERCONDUCTING NIOBIUM-TITANIUM

by

Shirley Ann Jackson

Submitted in Partial Fulfillment of the

Requirements for the Degree of

Bachelor of Science

at the

Massachusetts Institute of Technology

May, 1968

Signature of Author: _____
Department of Physics

Certified by: _____
The Thesis Supervisor

Accepted by: _____
Departmental Senior Thesis Committee -- Chairman

TUNNELING DENSITY OF STATES BEHAVIOR IN SUPERCONDUCTING NIOBIUM-TITANIUM

by

Shirley Ann Jackson

Submitted to the Department of Physics in partial fulfillment of the requirements for the Degree of Bachelor of Science on May 17, 1968.

ABSTRACT

Superconductor-insulator-superconductor tunneling junctions were fabricated consisting of three-sixteenth inch diameter cylindrical niobium-titanium alloy specimens (1-3/8 inches long), thermally grown oxide insulating barriers, and evaporated Indium thin films.

These junctions were used to study density of states behavior in the niobium-titanium alloy. Alloy specimens were of one composition: 80-20 weight percent niobium-titanium. Of twenty-two junctions prepared, five showed evidence of tunneling. Although no junction yielded a definite energy gap value for either superconductor used in junction fabrication, from I-V curves for these junctions, it was possible to infer probable tunneling events in agreement with expected gap values of 2.89 mV. for the niobium-titanium alloy and 1.07 mV. for the indium strips. An explanation of the absence of a definite energy gap negative resistance region in the I-V curves for the alloy is given in terms of oxide and surface effects. An alternate, hopefully more successful, method of junction fabrication is suggested.

TABLE OF CONTENTS

Section Number		Page Number
	ABSTRACT	2
	LIST OF ILLUSTRATIONS	4
	ACKNOWLEDGMENTS	5
I.	INTRODUCTION	
	A. History	6
	B. Tunneling	9
	C. Tunneling Effects	12
	D. Superconducting and Tunneling in Niobium-Titanium	16
	E. Sum and Difference Peaks	20
II.	EXPERIMENTAL PROCEDURE	
	A. Zone Melting	21
	B. Specimens with Thermally Grown Oxide	21
	C. Mounting	25
	D. Electropolishing	29
	E. Apparatus	
	1. Cryogenics	32
	2. Electrical	32
III.	CONCLUSIONS	
	A. Experimental Results	35
	B. Discussion	45
	C. Suggestions for Further Research	46
	REFERENCES	48

LIST OF ILLUSTRATIONS

Figure Number		Page Number
1 A.	Normal metal free electron density of states	8
1 B.	Superconductor bunching of states	8
2 A.	Superconductor-insulator-superconductor tunneling at $T = 0$ K	10
2 B.	Superconductor-insulator-superconductor tunneling at T 0 K	10
3.	Double Particle tunneling	13
4 A.	Josephson effect	15
4 B.	Metallic bridge short	15
4 C.	Niobium-titanium phase diagram	18
5.	High vacuum system	23
6.	Annealing furnace	24
7.	Oxidizing furnace	26
8.	Evaporation set-up	27
9.	Sample and sample holder	28
10.	Electropolishing set-up	31
11.	Cryogenics	33
12.	Tunneling circuit	34
13-20.	Tunneling graphs for five junctions	36-43

ACKNOWLEDGMENTS

The author is particularly indebted to Professor Robert M. Rose of the Department of Metallurgy and Materials Science for the suggestion of the thesis problem and for his unceasing confidence in her, his infinite patience, and many helpful discussions. The author also wishes to thank Mr. Irwin Puffer for his help in fabricating materials and Mr. Guenter Arndt for his assistance with electropolishing techniques. She also wishes to aknowledge the financial support of the research provided by the National Science Foundation under Grant GK-1073.

I. INTRODUCTION

A. History

Superconductivity was discovered in 1911 by H. Kamerlingh Onnes,[1] who observed that as mercury was cooled below a certain temperature (4.2°K), all measurable resistance disappeared. The temperature below which resistance disappeared was called the transition temperature, T_c, of the material. In 1935 Fritz London[2] proposed two-fluid phenomenological equations of superconductivity which allowed for the coupling of electrons leading to zero resistance below T_c. A modified two-fluid model, proposed in 1945 by V. L. Ginzberg[3] carried with it the idea of gap in the energy spectrum of superconducting electrons. In 1950 E. Maxwell[4] discovered the isotope effect, $T_c M^a$ = const., which showed a dependence of transition temperature on isotopic mass. This suggested that some interaction of electrons with lattice vibrations played a role in superconductivity. Furthering this development, in 1950 Cooper[5] showed that two electrons interacting just above the Fermi level with a net attraction between them can form a bound state lying below the Fermi level. He also showed that this led to an energy gap between the superconducting ground state and excited states.

Following the work of many before them, in 1957, J. Bardeen, L. N. Cooper, and J. R. Schrieffer[6] proposed the BCS theory of superconductivity. The basis of the theory is that there is a net attraction potential between electrons due to virtual phonon exchange resulting in Cooper pairs. This

causes an increase in the kinetic energy of the pairs over independent electrons, but this is overcompensated for in the binding energy due to pairing. According to BCS, an electron moves in a deformable lattice of positive charges, and in its movement causes a local deformation of the lattice and a "bunching up" of a charge. A second electron sees this favorable concentration of positive charge. So there is an attractive interaction between the electrons in addition to the Coulomb repulsion. If this net attraction is greater than the Coulomb repulsion, there exists the condition for electron pairing. The lowest energy of the paired states was shown to be when all pairs have the same momenta with opposite spins paired. This pairing gives rise to a gap in the electron energy spectrum, with the gap centered at the Fermi level: $2\varepsilon = 2\varepsilon_o[1 - \frac{T}{T_c}]^{1/2} \sim 3.52k\ T_c[1 - \frac{T}{T_c}]^{1/2}$. The width of the gap equals the energy necessary to break up one of the pairs. The free electron density of states goes as $E^{1/2}$ and is as shown in Figure 1A. At 0°K all electron states up to the Fermi level, E_f, are filled. Those above this are empty. At T > 0°K there are thermally excited electrons above E_f (Figure 1A). The diagrammatic model of the energy spectrum of a superconductor is the normal metal electron spectrum modified by an energy gap at the Fermi level, which causes a bunching of the Fermion spectrum on either side of the gap. As a matter of fact, this bunching has been calculated to be:[7]

$$\frac{dN(E)}{dE} = \frac{dN(\varepsilon)}{d(\varepsilon)} \frac{d\varepsilon}{dE} = N_o / \frac{dE}{d\varepsilon}$$

but $E = \varepsilon^2 + \text{e}^2$

$$\frac{dN(E)}{dE} = N_o \frac{E}{\sqrt{E^2 - \varepsilon^2}}$$, see Figure 1B.

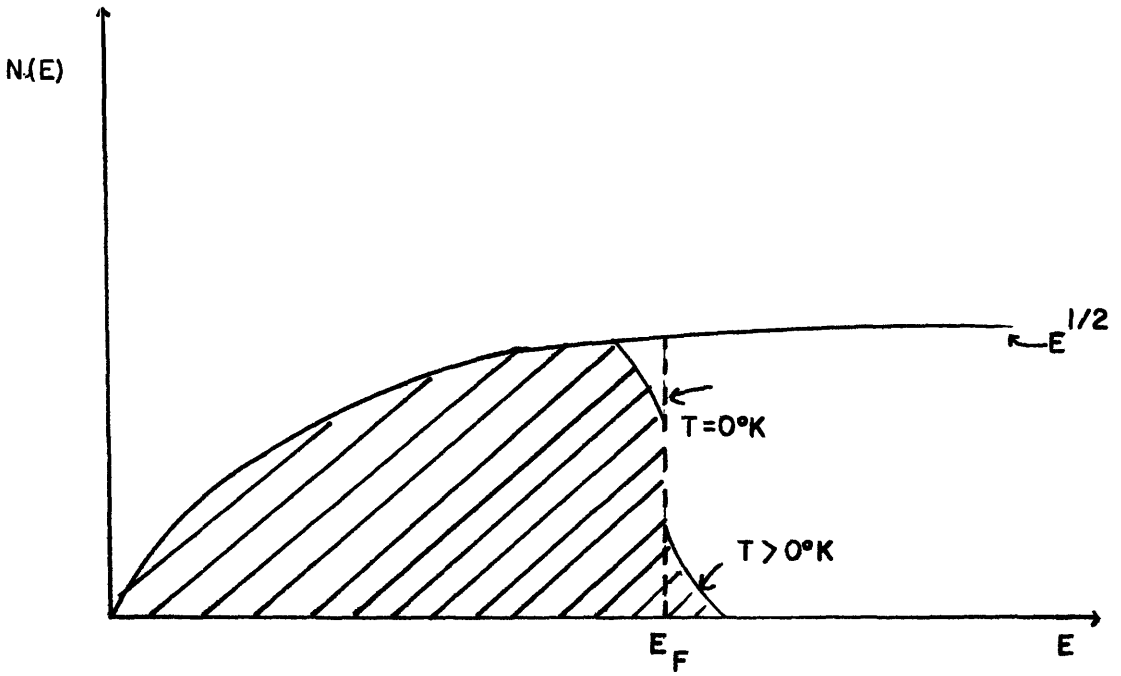

1A

Normal Metal Free Electron Density of States

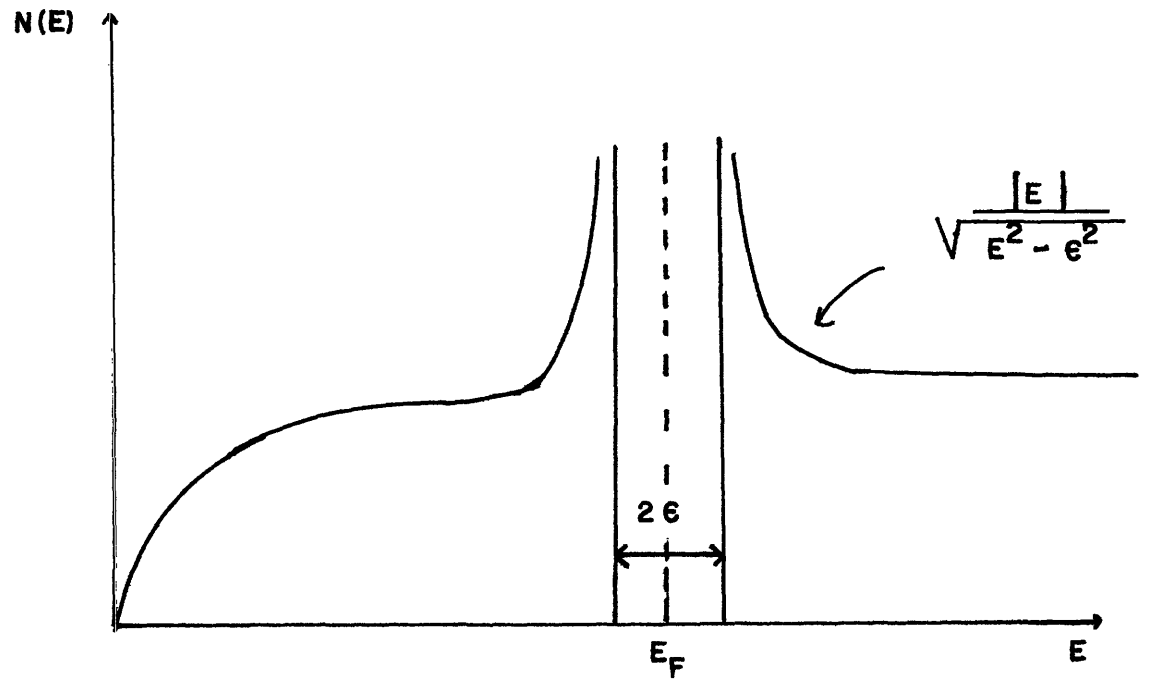

1B

Bunching of States in a Superconductor

where N_o is the density of states at the Fermi level in a normal metal.

B. Tunneling

If one has two superconductors (one with an energy gap less than the other) separated by an insulating barrier, we have the situation shown in Figure 2. Quantum mechanics predicts tunneling across the barrier if it is thin enough. The interpretation of the situation also hinges on the assumption that the transition probability for tunneling is proportional to the Fermion density of states in a superconductor, which has been shown to be reasonable by Bardeen.[8]

Tunneling can occur if there are electrons available for tunneling on one side of the barrier and empty states to receive these electrons on the other side of the barrier. Applied voltages can shift one energy spectrum relative to the other in order to create situations favorable for tunneling. The transmission factor[12] for the tunneling of a quantum particle through a barrier depends exponentially upon the barrier thickness and the square root of the barrier height. For small voltages, the barrier thickness is not varied significantly. Mathematically the tunneling current is:

$$I \alpha \quad |M|^2\{\rho_2(E - V)f(E - V)\rho_1(E)\ [1 - f(E)] - \rho_2(E - V)\ [1 - f(E - v)]\ \times$$

$$\rho_1(E)f(E)\ \ dE.$$

where $\rho(E) = N_o \dfrac{(E)}{\sqrt{E^2 - \epsilon^2}} \qquad |E| \geq \varepsilon(T)$

$$\rho(E) = 0 \qquad |E| < \varepsilon(T)$$

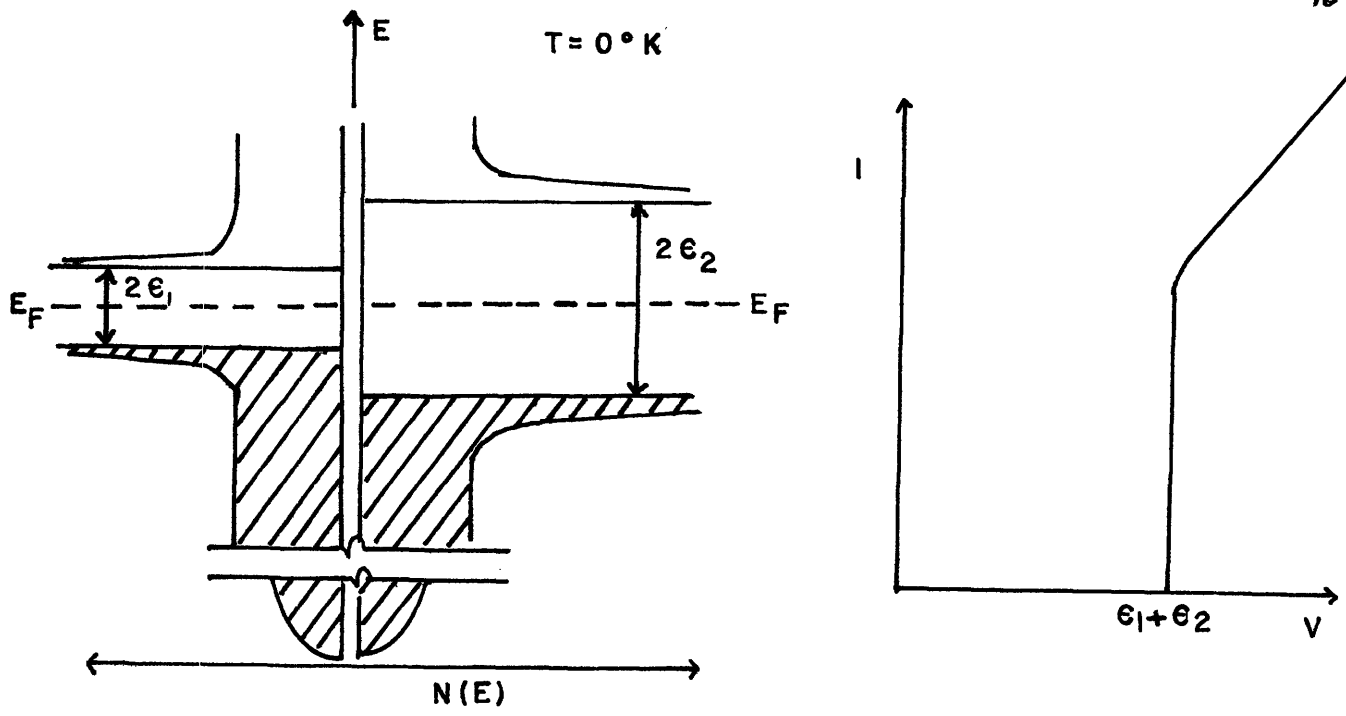

2A

Superconductor-Insulator-Superconductor

Tunneling

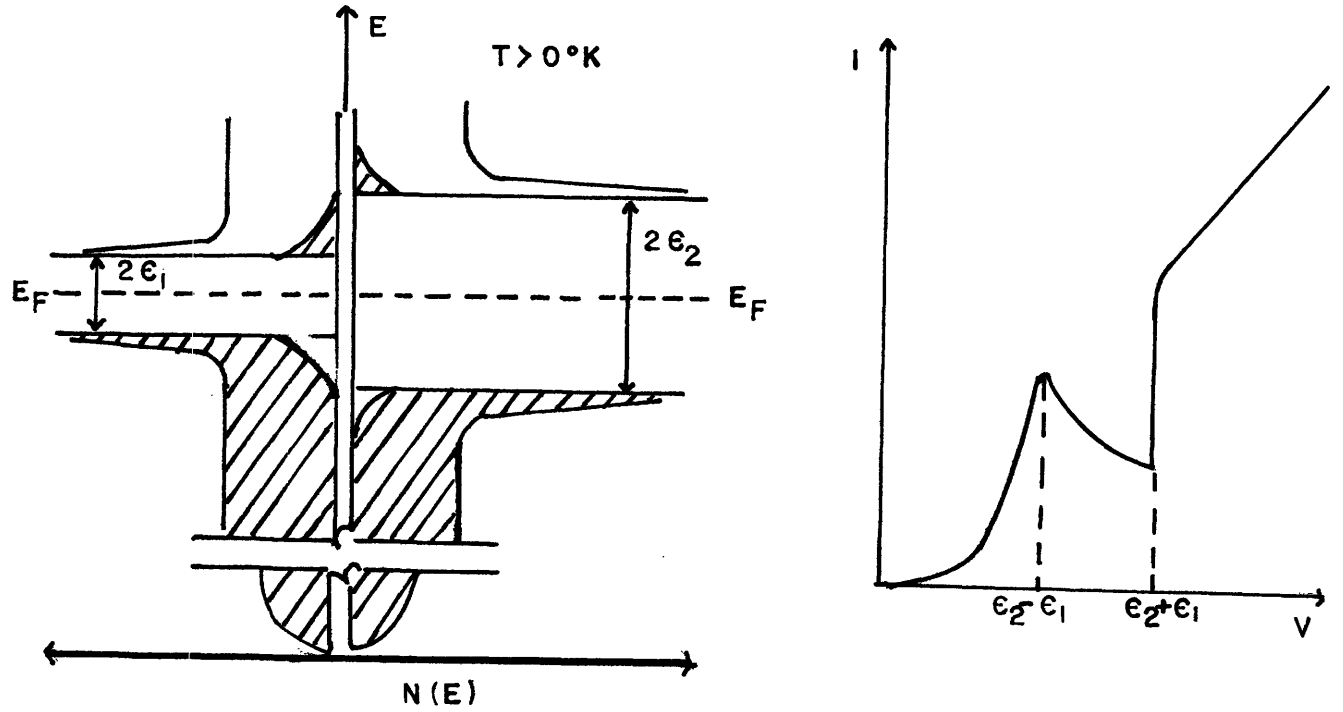

2B

$|M|^2$ is the matrix element for the transition and f(E) is the occupation probability for a state of energy E. So for the current, one gets: $I = \text{const.} \times \rho_2(E - V)\rho_1(E) \{f(E - V) - f(E)\} dE$.

There are fewer thermally excited electrons above the energy gap for the larger gap superconductor. So the smaller gap superconductor can act as a probe of the large gap material since, in the region of interest, there will be more current flowing from the smaller to the large gap superconductor than vice versa, and this current sharply samples the density of states in the larger gap material (as will be seen below).

At 0°K (Figure 2A) there is no current flow until the applied voltage equals $\varepsilon_2 + \varepsilon_1$. The current increases very rapidly, monotonically beyond this point and eventually becomes ohmic since far away from the gap the energy spectrum of each superconductor behaves like that of a normal metal. (Figure 2A) At finite temperatures (Figure 2B), current will flow at small voltages. The current will increase until the applied voltage reaches $\varepsilon_2 - \varepsilon_1$. Beyond $\varepsilon_2 - \varepsilon_1$, there is an increase in voltage, but since the tunneling electrons face a less favorable density of states, current decreases with increasing voltage until the applied voltage equals $\varepsilon_1 + \varepsilon_2$, at which point the current increases rapidly with applied voltage and eventually approaches the characteristics of a normal metal (Figure 2B). The difference between the sum $\varepsilon_2 + \varepsilon_1$ and difference $\varepsilon_2 - \varepsilon_1$ points yields $2\varepsilon_1$. From this one gets $2\varepsilon_2$. Thus we have a direct measurement of the energy gap of both superconductors. The I-V curve itself traces out generally the relative density of states behavior of the two superconductors.

C. Tunneling Effects

1. Single Particle Tunneling

The model discussed above essentially accounts for single particle tunneling effects. The applied voltage can be considered the energy necessary for electron pairs to split. One electron goes into an excited state in the same superconductor, while the other tunnels through the barrier to an available state in the second superconductor. At low temperatures there are fewer thermally excited electrons above the Fermi level. Consequently the difference peak, $\varepsilon_2 - \varepsilon_1$, becomes less evident. Thus, there may be some ambiguity in determining gap values from this peak.

2. Double Particle Tunneling

At low temperatures another effect, first observed by Burstein and Taylor,[9] may become apparent. This phenomenon is known as double particle tunneling. It may occur at the half gap values of one or both of the superconductors on opposite sides of the insulating barrier. (See Figure 3.) It was explained by Schrieffer and Wilkins[10] in the following two ways: (1) Two pairs of electrons split in one of the superconductors, S_1, and two electrons (one from each pair) tunnel across at $V = \varepsilon_1(T)$, the half gap value of that superconductor into the second superconductor, S_2. There, the electrons may recombine or enter empty quasi-particle states; (2) An electron pair can tunnel from one of the superconductors, say S_1, into the second superconductor, S_2, and split to fill two quasi-particle states there. This would occur at $V = \varepsilon_2(T)$, the half gap value

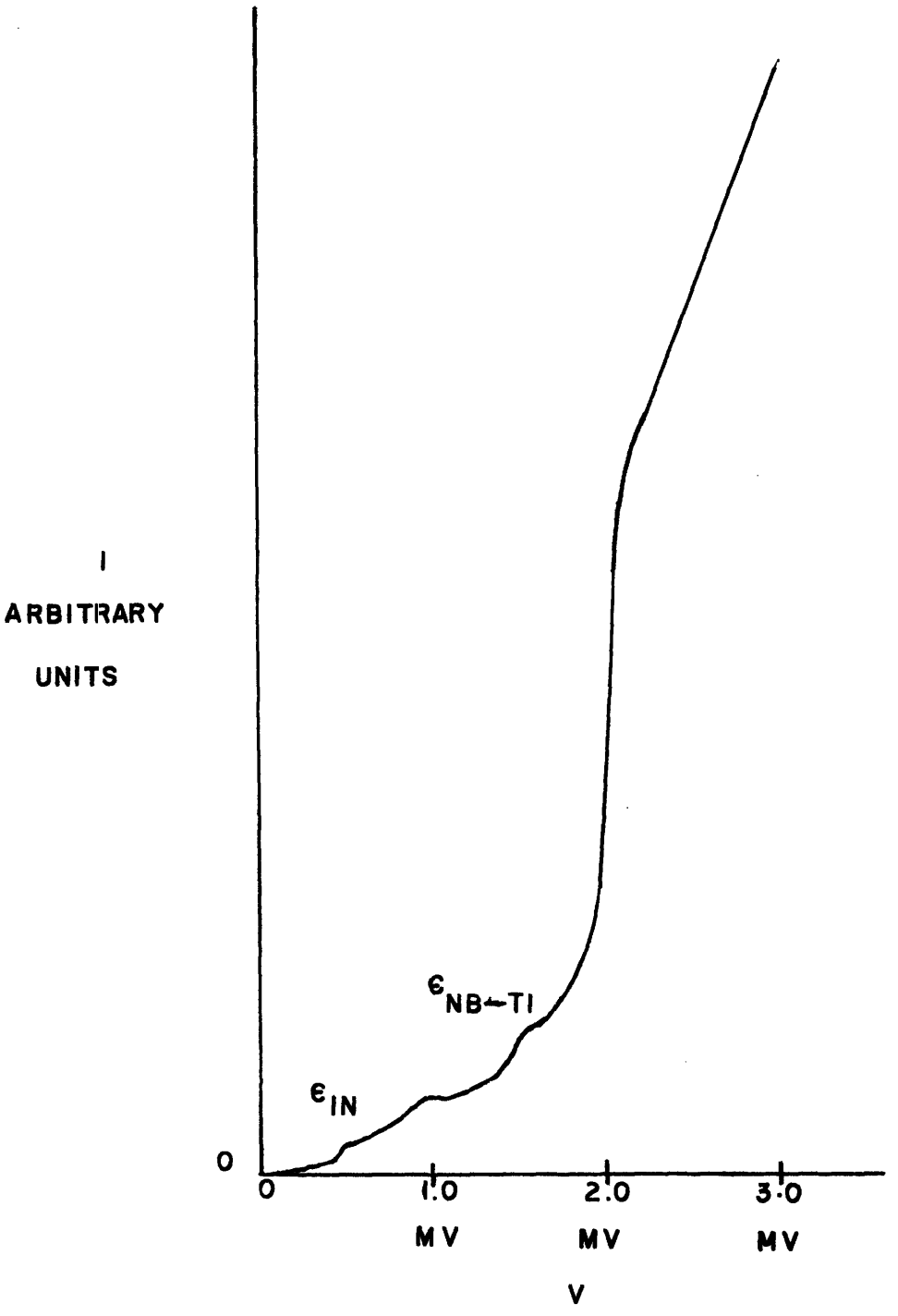

3

Double Particle Tunneling

of the second superconductor since that is where the pair splits. According to Taylor and Burstein,[11] since double particle tunneling involves the simultaneous tunneling of two electrons, the matrix element for this transition will depend on the square of the matrix element involved in single particle tunneling. The exponential dependence of the double particle tunneling current is greater than that for single particle tunneling. Consequently, the thinner the oxide, the more forward is double particle tunneling. This process is also found to be temperature independent.

3. The DC Josephson Effect

This phenomenon, first predicted by Josephson[11] involves the tunneling of Cooper pairs, i.e., the direct passage of coherent pairs from one side of the insulating barrier to the other. If the barrier is thin enough so that wavefunctions for the superfluid electrons overlap so as to correlate, then pairs of electrons can flow across the barrier without the creation of quasi-particles (i.e., no breakup of pairs). Given the necessary condition of a thin enough barrier, at zero voltage, there will be a net current across such a junction. With increasing voltage the current increases to a maximum value at which points the other tunneling events take over (see Figure 4A).

4. Other Effects

Other phenomena which could be observed in a tunneling experiment involve either shorting through the oxide or effects due to oxide thickness. A curve for a junction with a metal bridge short would appear similar to the Josephson curve except when the voltage is retraced the

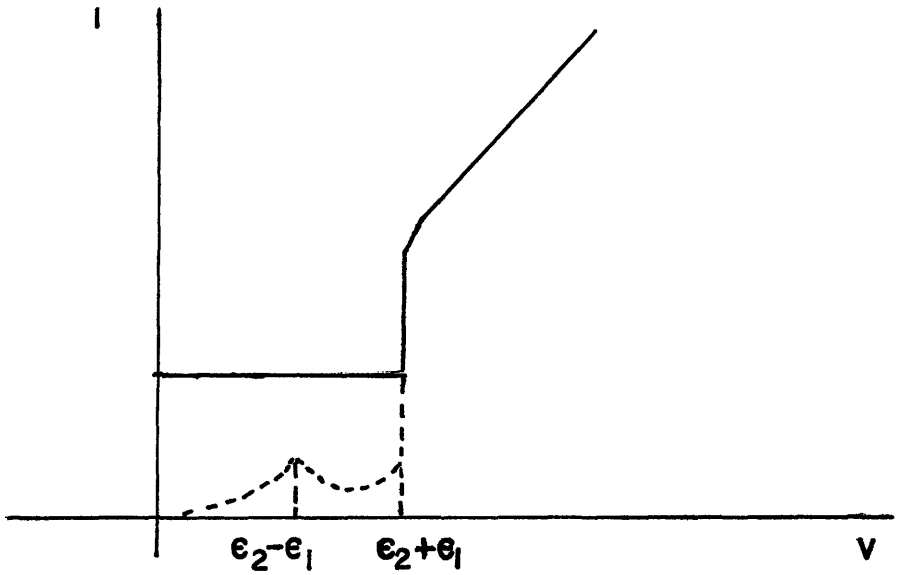

Josephson Effect

4A

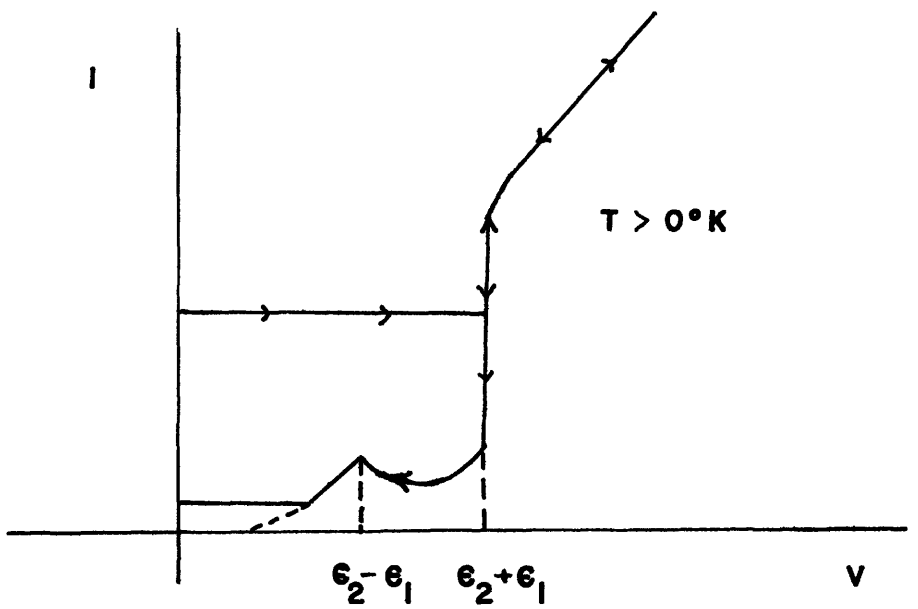

Metallic Bridge Short

4B

bridge would remain normal at a lower current density due to Joule heating[13] (see Figure 4B). The curve for a specimen with small holes in the oxide would exhibit erratic behavior due to a combination of shorting current and regular tunneling current. M. MacVicar[14] noted the appearance of background current in the curves for some specimens, which was attributed to oxide preparation and thickness. This effect was loosely related to an effect noted by Taylor and Burstein[11] (although they offered no real explanation for the effect) whereby current was observed to depend exponentially on applied voltage.

D. Superconductivity and Tunneling in Niobium-Titanium

Superconductivity in transition metals has been discussed in several places[16,17,18] (and others besides these listed). Matthias,[18] from his investigations on many elements, compounds, and alloys, has noted that for elements with unfilled d-shells, transition elements, superconductivity occurs when there are about 3, 5 and 7 valence electrons per atom. Each of these transition temperature peaks (the highest being at 5 valence electrons per atom) has, on each side of it, a valley of normal or weakly superconducting behavior. Blaugher and Hulm[19] have suggested that this peaking is connected with peaks in the density of states at the Fermi surface and that peaks in the density of states have been identified from heat capacity experiments.[19] Blaugher and Hulm further suggest that the curve of density of states vs. energy in the d-band has the same general shape for all the transition elements. Hence, as the d-band is filled up by the addition of extra electrons in moving across the periodic table, the electronic properties would fluctuate according to the shape of the general density of

of states curve.

Therefore, it would seem that in mixing two transition elements, the electronic properties would depend on the shape of the general density of states curve between the two elements, since the d-band would be filled to an intermediate point. It would seem further that the general density of states curve would be applicable if the two elements combined to form an intermetallic compound with a structure the same as that of the parent elements.

The niobium-titanium alloy used in this thesis is 80-20 weight percent niobium to titanium. This alloy is a body-centered cubic, solid solution material (see phase diagram) having been formed from β-titanium (BCC) and niobium (BCC). Using a simple formula to convert weight percent to atomic percent and using the fact, pointed out by Blatt,[20] that the average number of valence electrons per atom can be taken as a simple linear average of constituent substances, it is possible to calculate the average number of valence electrons per atom for this alloy.

$$\text{Atomic percent niobium} = \frac{W_{Nb}/AW_{Nb}}{W_{Nb}/AW_{Nb} + W_{Ti}/AW_{Ti}} = \frac{.8/92.9}{.8/92.9 + .2/47.9}$$

$$= \frac{.0086}{.01276} = \frac{86}{127.6} = .672 = 67.290.$$

Atomic percent titanium = 32.8%.

$$n = (.672)5 + (.328)4 = 3.36 + 1.312 = 4.672 = 4.67.$$

Where W_x = weight of element x

AW_x = atomic weight of element x

n = average number of valence electrons per atom.

So, as assumed previously, one would expect superconductivity in this alloy (which is easily observed) at a temperature near the maximum transition temperature observed for a niobium-titanium alloy (T_c = 9.6°K). The

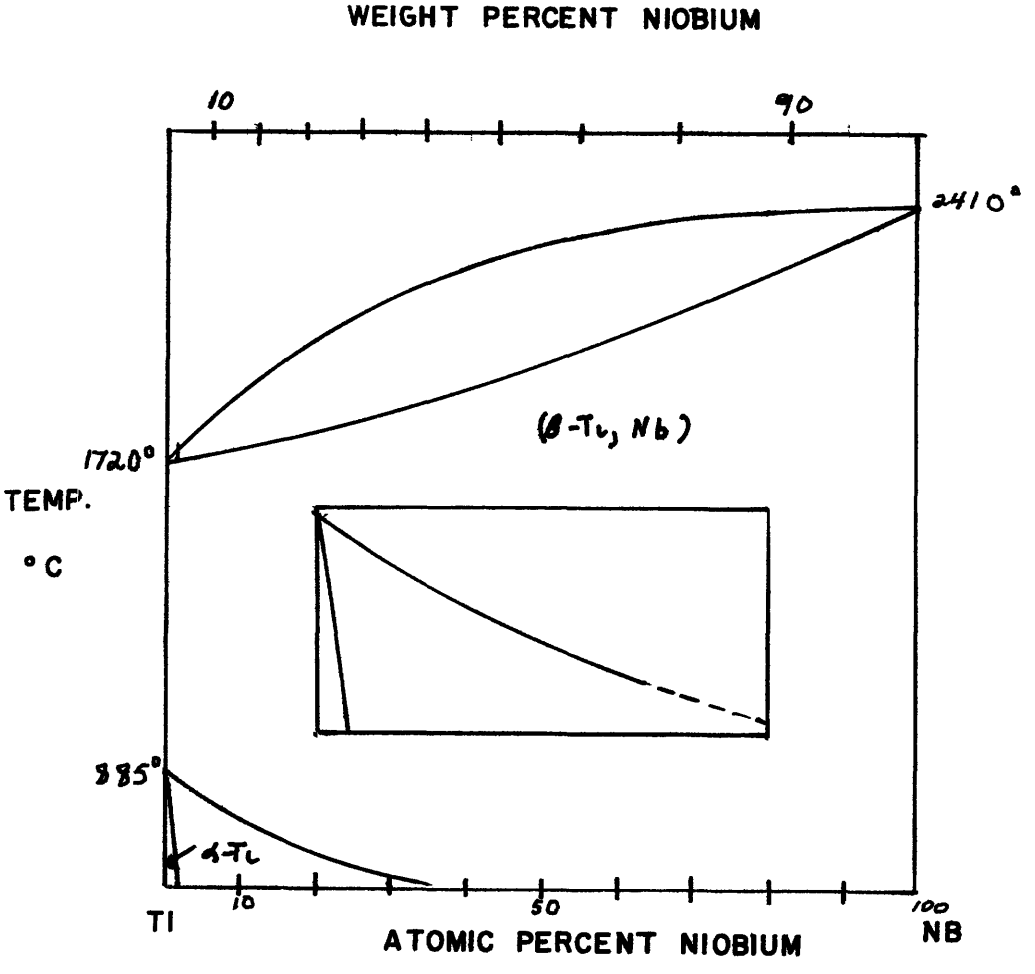
WEIGHT PERCENT NIOBIUM
10
90
2410°
(β-Ti, Nb)
1720°
TEMP.
°C
885°
α-Ti
10
50
100
TI
NB
ATOMIC PERCENT NIOBIUM

4C

transition temperature for this alloy is $T_c = 9.5°K$. This gives a BCS expected gap value of $2\varepsilon_o = 3.52\, \ell_B T_c$, $2\varepsilon_o = 2.89$ eV. The temperature dependence of the gap, if assumed to obey BCS theory, would be $2\varepsilon = 2\varepsilon_o(1 - \frac{T}{T_c})^{1/2}$.

So, given that this alloy is a transition metal with the number of valence electrons per atom required for superconductivity at this composition, it is very interesting to study the density of states behavior of this alloy as a prerequisite of a general study of the variation of general density of states behavior as a function of number of valence electrons, hence a study of variation of Fermi surface structure. A tunneling density of states study is a good way to get at this problem and if tunneling junctions are successfully fabricated, it is possible to obtain an energy gap value for the alloy.

What must be pointed out here is that the assumption that the density of states picture and BCS model, described for a normal superconductor, may not work at all for a transition metal superconductor and for an alloy at that. Indeed, the isotope effect, which led to the BCS theory does not hold for transition metals, indicating that the idea of a lattice interaction as a cause of superconductivity may not be applicable. Nevertheless, a tunneling experiment, which does sample density of states behavior, is a good way of getting at this difficulty.

The transition temperature of indium is 3.41°K. It has been observed to vary with film thickness as: $T_c = (3.41 + \frac{52}{d} - \frac{750}{d^2})°K$. For my films of approximate thickness 3000 Å, this gives:

$T_c = (3.41 + 17.3 \times 10^{-3} - 83.3 \times 10^{-6})°K \approx 3.41°K$. This yields a BCS energy gap for indium of $2\varepsilon_o = (3.52)(1.381 \times 10^{-16}$ erg/°K) (3.41°K) = 16.6×10^{-16} erg $2\varepsilon_o = 1.07$ meV.

E. Sum and Difference Peaks

Using the calculated values of the energy gaps for the niobium-titanium alloy and indium, we get as difference and sum peaks:

$\varepsilon_2 - \varepsilon_1 = (1.45 - .535)$meV : 915 meV

$\varepsilon_2 + \varepsilon_1 = 1.45 + 5.35 = 1.985$ meV.

Therefore, on the I-V curves for my specimens, one would expect structure at or near .915 mV and 1.985 mV. There could also be structure at .535 mV and 1.45 mV if double particle tunneling were going on.

II. EXPERIMENTAL PROCEDURE

A. Zone Melting

A molten zone was passed along a rod of 3/16 inch diameter (1-3/8 inches in length) 80-20 weight percent niobium-titanium by electron bombardment in a vain attempt to obtain single crystals of the alloy. This attempt failed when molten metal fell onto the emitting filament and shorted out the electron gun. This was in all probability due to the great difference in melting temperatures of niobium (2415°C) and titanium (1820 $\pm$ 100°C). Since the alloy was heated at the melting temperature of niobium, the titanium had begun to evaporate by the time the niobium was just becoming molten. It was felt that there was a slim chance of success because the alloy composition was heavily weighted in favor of its being predominantly niobium. There has been some measure of success in fabricating large grains of single crystal niobium-titanium alloy by a strain-anneal technique.[15] These grains are large enough to be each effectively used as single crystal samples. These efforts were abandoned by the author since it was considered more important, as a first step, to obtain an average gap value and density of states information for the polycrystalline material.

B. Specimens with Thermally Grown Oxide

The most successful specimens were prepared in the manner outlined below. Indeed, the only specimens which yielded data worth of comment were some of those prepared in this way.

A three-quarter inch diameter rod of niobium-titanium rod (80-20 weight percent) was obtained from Dr. John Wulff, Department of Metallurgy and Materials Science, M.I.T. The rod was obtained by him from the NRC Division of the Norton Company. The rod was swaged down to a diameter of slightly over three-sixteenths of an inch. A section of this, usually eight inches in length, was machined on a lathe down to a few thousandths of an inch greater than three-sixteenths inch. The section was then polished mechanically on the lathe with polishing paper ranging in coarseness from 400 to 40. The rod was then removed from the lathe and polished on a jeweler's wheel with jeweler's dust until it was smooth under microscope magnification of 40X. The rod was then cut with a jeweler's saw into specimens 1-3/8 inches long. Each specimen was then annealed in high vacuum (10^{-8} torr) for 8 hours at temperatures ranging from 1200°C to 1350°C. The annealing vacuum system consisted of a 400 liter/second ion pump, a titanium boostivac unit, and two Vac-sorb roughing pumps. The rest of the system was comprised of a 12-inch glass bell jar with a collar and L-gasket (see Figure 5) seal. The annealing furnace consisted of a cylinder of pure niobium which acted as a radiator when heated from both ends (see Figure 6), by electric current. Temperature was measured by optical pyrometer and a Pt-Pt(Rh) thermocouple.

The vacuum system, with specimen in it, was pumped down overnight so that it was in the mid 10^{-8} torr range. The sample was then heated up to the desired temperature and allowed to remain at this temperature for 8 hours. The system was then cooled for 2 hours and then backfilled to atmospheric pressure with dried nitrogen gas. The sample was then removed and oxidized in an oxygen flow-tube furnace for 15 to 45 minutes at

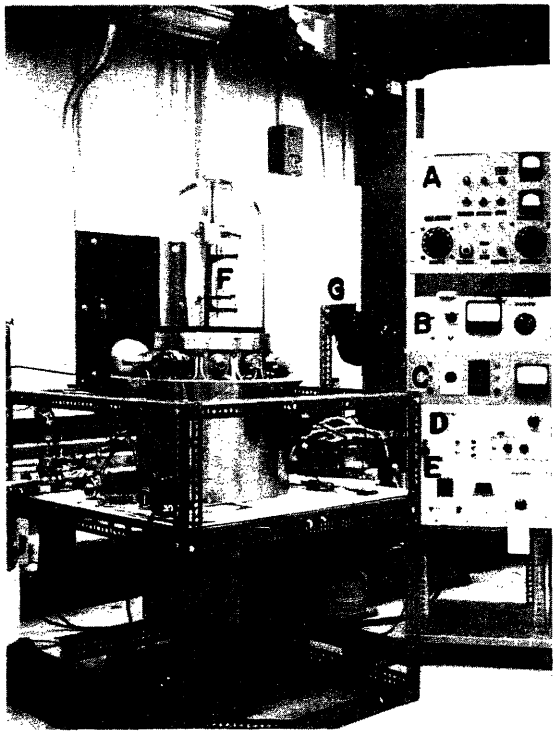

A. ELECTRON BEAM CONTROL PANEL
B. TITANIUM BOOSTIVAC CONTROL PANEL
C. THERMOCOUPLE GAUGE
D. ULTEK ION GUAGE
E. ULTEK ION PUMP CENTRAL PANEL

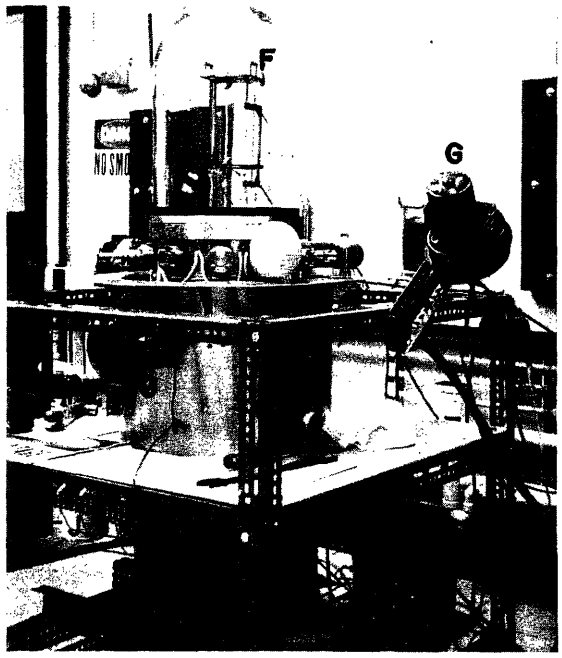

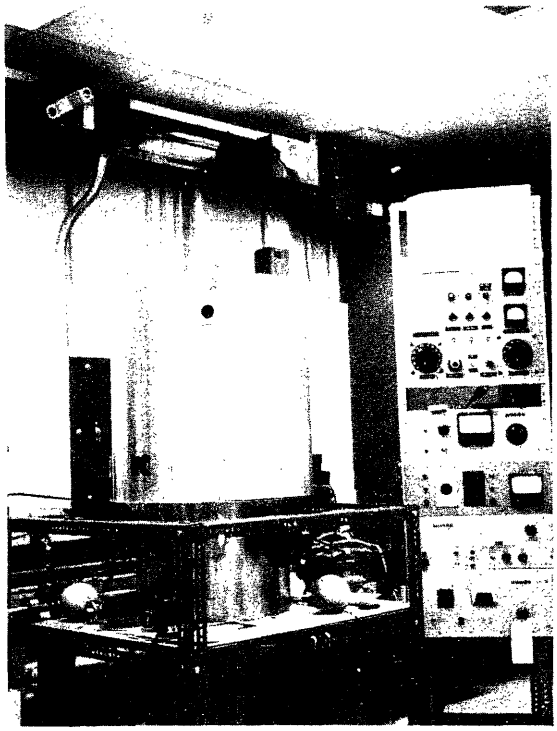

F. ELECTRON GUN ASSEMBLY
G. BLOWER MOTORS
H. ION PUMP
I. HEATER AND TRAVERSE CONTROLS
J. VARIAN VACU-SORB PUMPS
K. MANTEL
L. PHILIPS-GRANVILLE VALVE

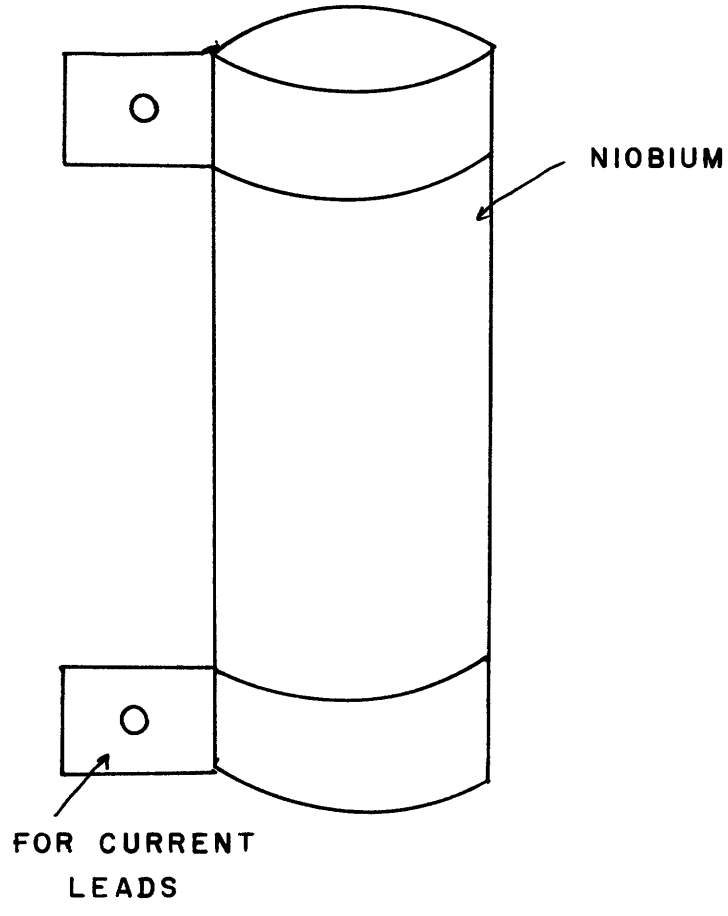

Annealing Furnace

temperatures ranging between 100°C and 115°C (see Figure 7).

After oxidation, the ends of the specimen were dipped in a 3 percent formvar solution for masking prior to the deposition of evaporated In. The space between the formvar masking was approximately 3/4 inch. Length of time in air for the specimens was usually approximately 20 minutes. The most important air-exposure time was probably that before furnace oxidation (usually on the order of 5 minutes).

Stripes of 99.9999 percent pure indium were evaporated at pressures around 3×10^{-5} torr from an alumina crucible sitting at the bottom of a cylindrical glass chimney. A shutter covered a slit, of variable width, in the top of the chimney (see Figure 8). Stripes of 3000 ± 1000 Å thickness were evaporated at a rate of about 90 Å/second. Stripes were usually 8 to 10 mils in width. There were 2 to 6 stripes on each specimen, parallel to the cylinder axis.

C. Mounting

The specimens were mounted in nylon sample holders (see Figure 9). A four-point electrical contact method was used. Two 5 mil gold leads were attached with silver paint to each stripe. Common voltage and current leads were 10 mil nickel wires soldered to the sample holder and spot-welded to one end of the sample. Five mil gold leads were chosen because of their ductility as well as electrical conductivity.

The samples made from the 80-20 weight percent alloy were oxidized in the manner described because of the success of M. MacVicar[16] with the technique in the oxidation of niobium specimens. It was felt that the

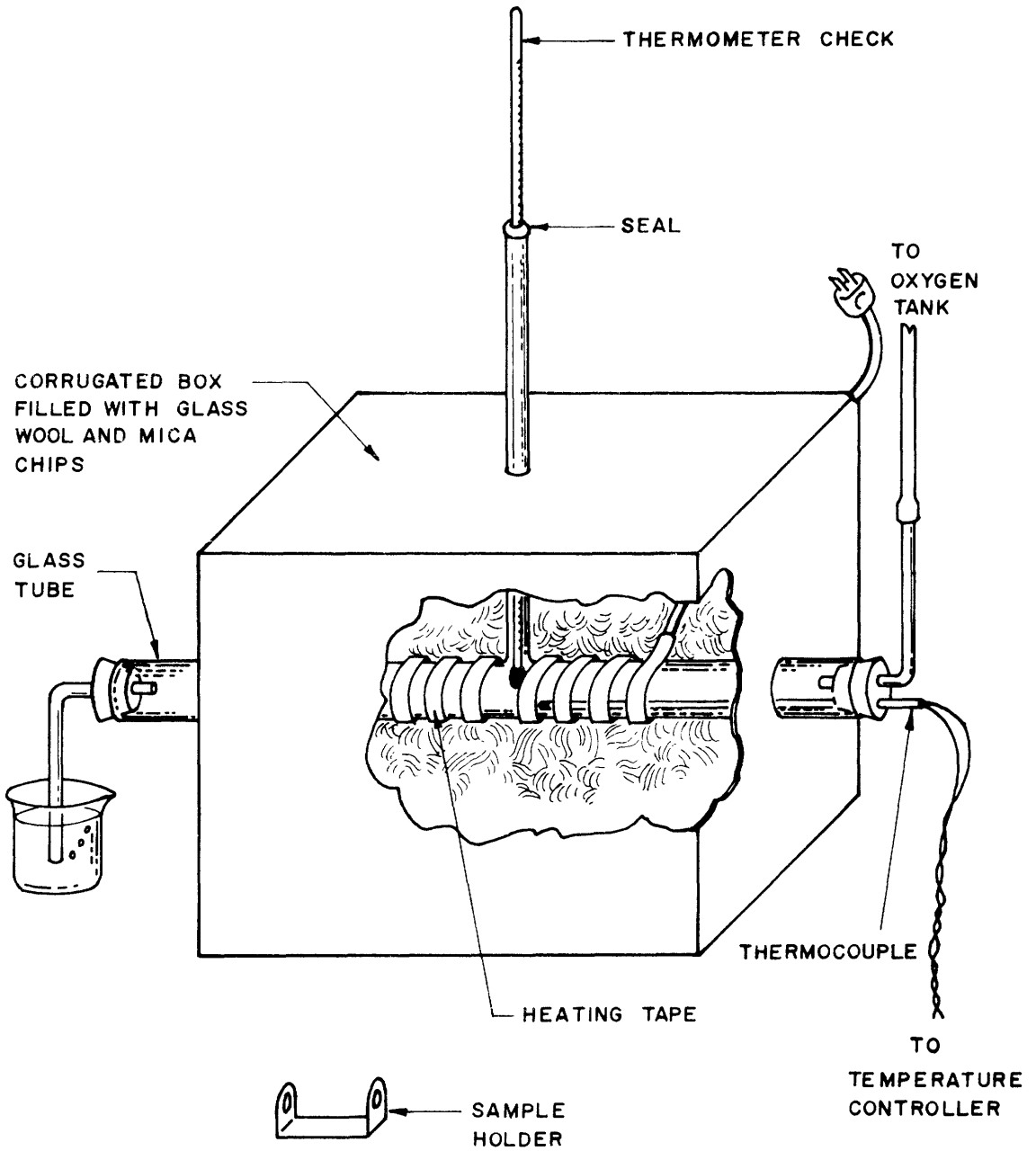

Oxidizing Furnace

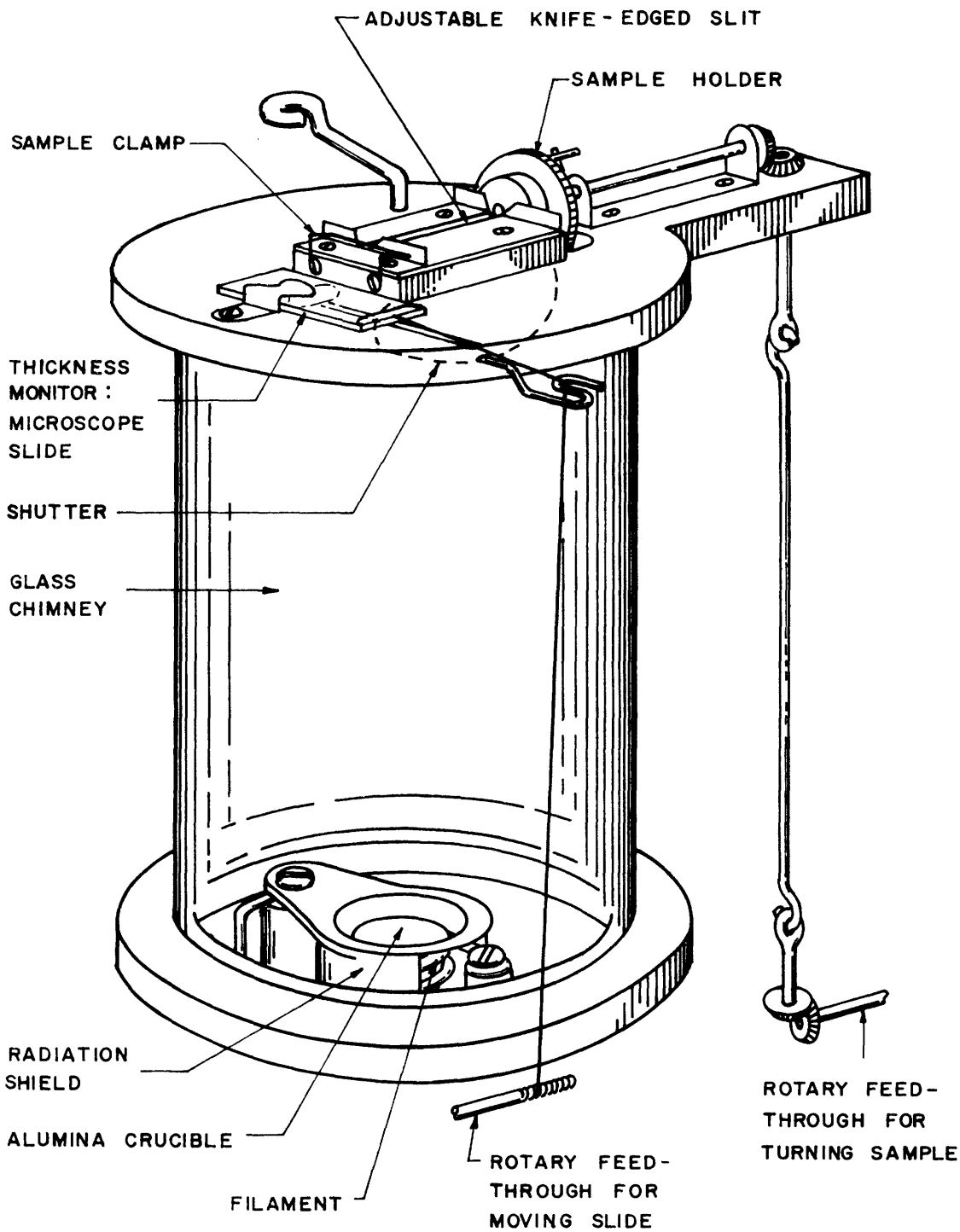

Evaporation Set-Up

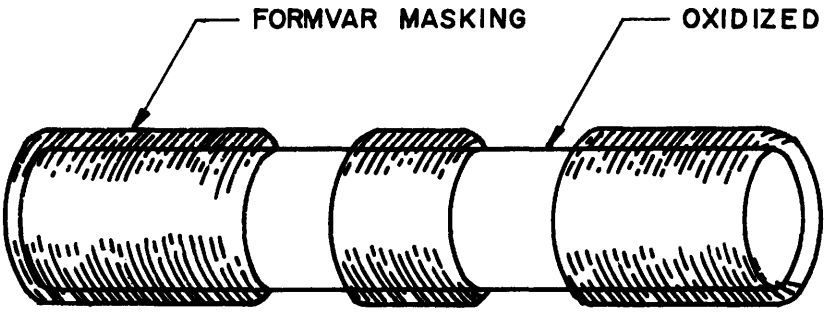

A.

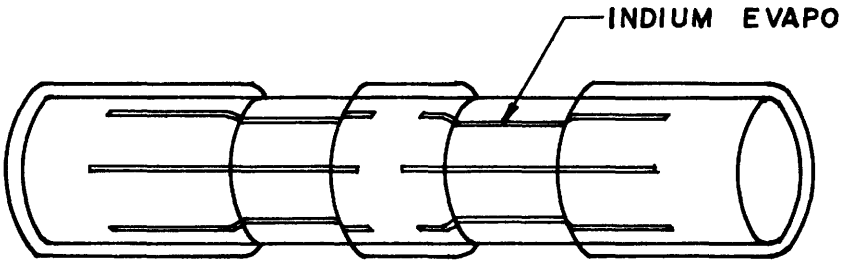

B.

Sample and Sample Holder

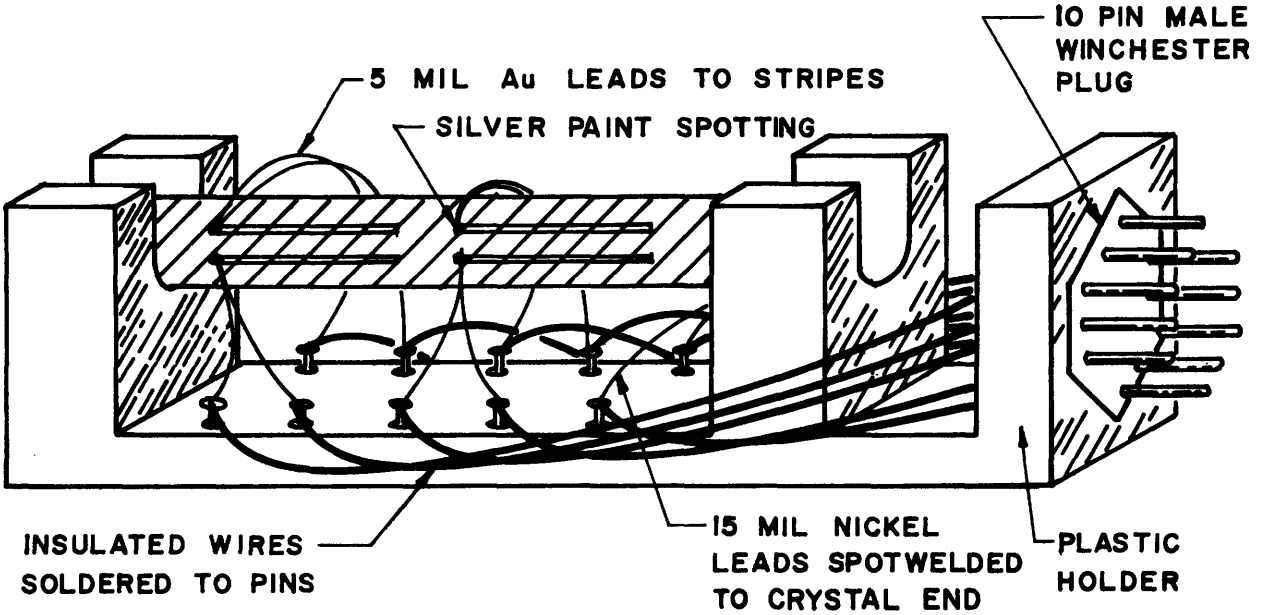

C.

technique or some take-off thereof would be the most logical approach to sample preparation. The specimens were annealed as described for two reasons. First it was felt that the anneal would help smooth out the surface of the sample. Second, it was felt that there was a slim chance that the heat treatment would break up some of the oxide undoubtedly formed on the specimen from the heat of friction during the mechanical polish. If so, it was possible to infer from Nb-O and Ti-O phase diagrams that some of the oxygen might go into solid solution in the alloy (even though the oxygen addition could alter slightly the superconducting properties of the alloy). This idea diminished in plausibility when the stability of titanium oxides was considered, but it was felt that the technique was worth a try (the proof is in the pudding!). Homogenization of the alloy was also a consideration since if the niobium and titanium were clustered, there would be a possibility of preferential oxidation since titanium has a greater affinity for oxygen than does niobium.

D. Electropolishing

Because of the inherent difficulties with the mechanical polishing and thermally grown oxide technique, another possible method of sample fabrication came to mind, electropolishing. Electropolishing involves the idea of anodic dissolution. The protruding ridges and peaks of a ground specimen surface are removed by preferential solution of metal. The valleys between the ridges are either completely protected from anodic solution by reaction products formed or by the rate of dissolution being much less than at the ridges or high points. The solution of specimen metal during the process gives rise to the formation of a boundary layer or film of

electrolyte immediately adjacent to the specimen surface which is of a different composition and of higher electrical resistance than the remainder of the electrolyte. Metal from the ridges goes into solution faster than metal from more depressed regions. This differential causes gradual smoothing out, or polishing, of the ground surface. (See Figure *10*.)

The motivation behind the electropolishing technique was that the sample surface could be smoothed without resort to mechanical polishing, hence, no friction heating. Also one assumes that if the surface of the alloy polishes, then any oxide formed from mechanical polishing would have had to have been broken down by the electrolytic reaction. The electrolyte for the polishing consisted of 90 cc. of pure ethyl alcohol, 10 cc. of n-butyl alcohol, 28 grams of anhydrous zinc chloride ($ZnCl_2$) and 6 grams of anhydrous aluminum chloride ($AlCl_3$). A power supply was designed and built which passed 150 milliamperes of current at a potential of 20 volts between the anode and cathode. This desired voltage and current setting was settled upon after much experimentation with settings to obtain the desired polishing. The anode was the specimen and the cathode was a 10 mil stainless steel sheet bent into a cylindrical form to match the geometry of the sample and placed in the electrolyte in a plastic beaker. The electrical connections to the anode were designed so that they supported the specimen at the right level in the electrolyte. Polishing usually took between 15 to 35 minutes. There was considerable difficulty in getting the technique to work because of troubles ranging from no polishing at all because of the presence of strontium chromate, an anodic inhibitor, in the original solution, to overpolishing (pitting) because of excessive current through

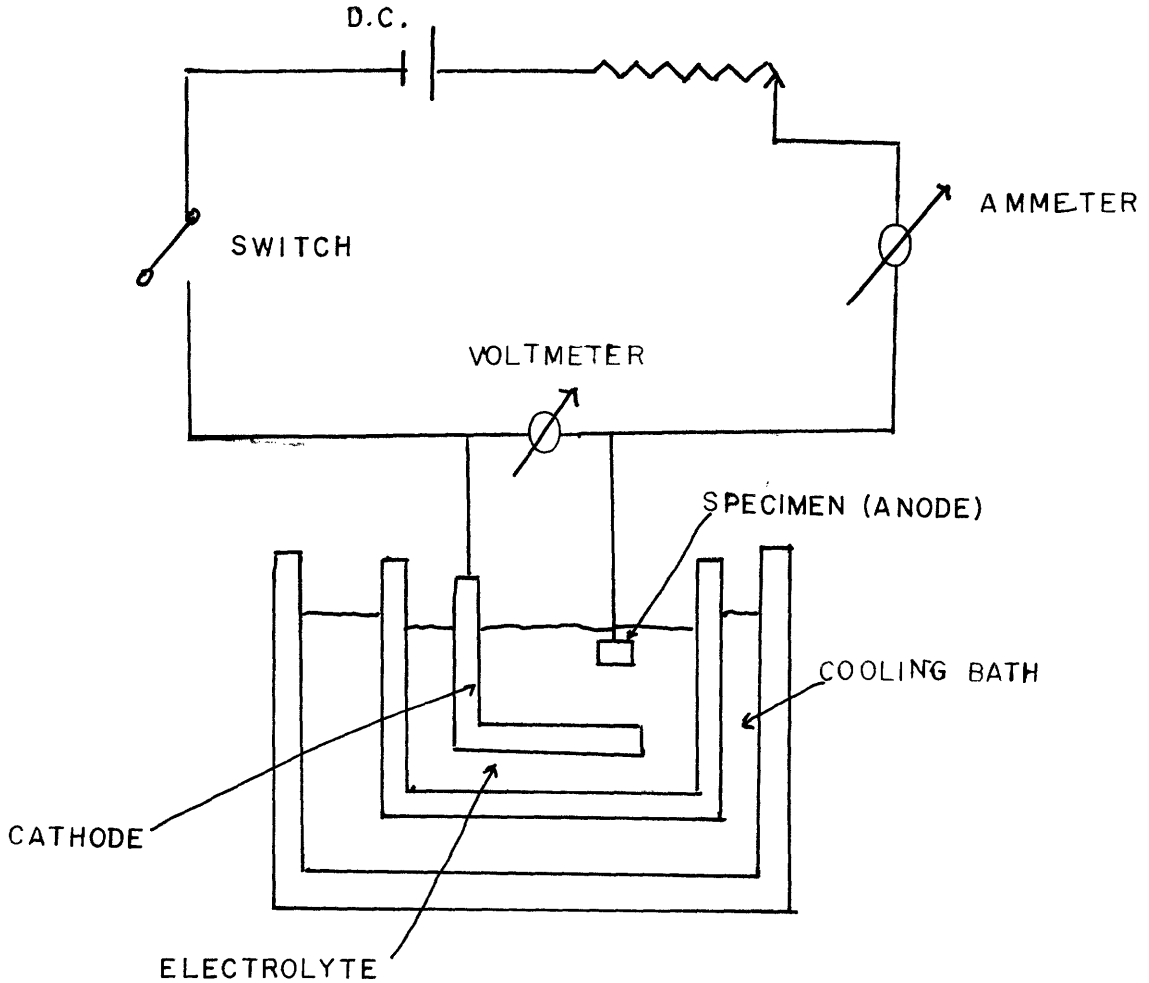

Electropolishing

10

the system. The sample which was finally polished took 30 minutes to polish. It was then immersed for 5 minutes in a weak hydrogen peroxide solution (5 ml. of H_2O_2 to 250 ml. of distilled water) to oxidize it initially and to clean off contaminants from electropolishing. It was then blown dry with pure oxygen gas. After this, the evaporation of Indium and the rest of the fabrication technique proceeded as discussed previously. This sample was tested for tunneling. Results are discussed in a later section.

E. Apparatus

(1) Cryogenics

The system was pumped on by a 140 cfm Stokes mechanical pump. Temperature was measured in terms of pressure from a gauge for which there was a temperature-pressure conversion table. The system was capable of reaching about 1°K with the sample in the liquid helium. The header was a 3/8 inch brass plate with plugs to the electrical connections, and vacuum-feed-throughs for the insulated copper leads running into the liquid helium; the leads being inside a copper-nickel tube which also supported the sample holder. Pressures were always 35 mm. or below, giving temperatures of 2.1°K or below. (See Figure 11.)

(2) Electrical

Because of the negative resistance region in the I-V curves the tunneling circuit had to have a very low impedance relative to the junction resistance. The circuit used was the one shown in Figure 12.

Cryogenics

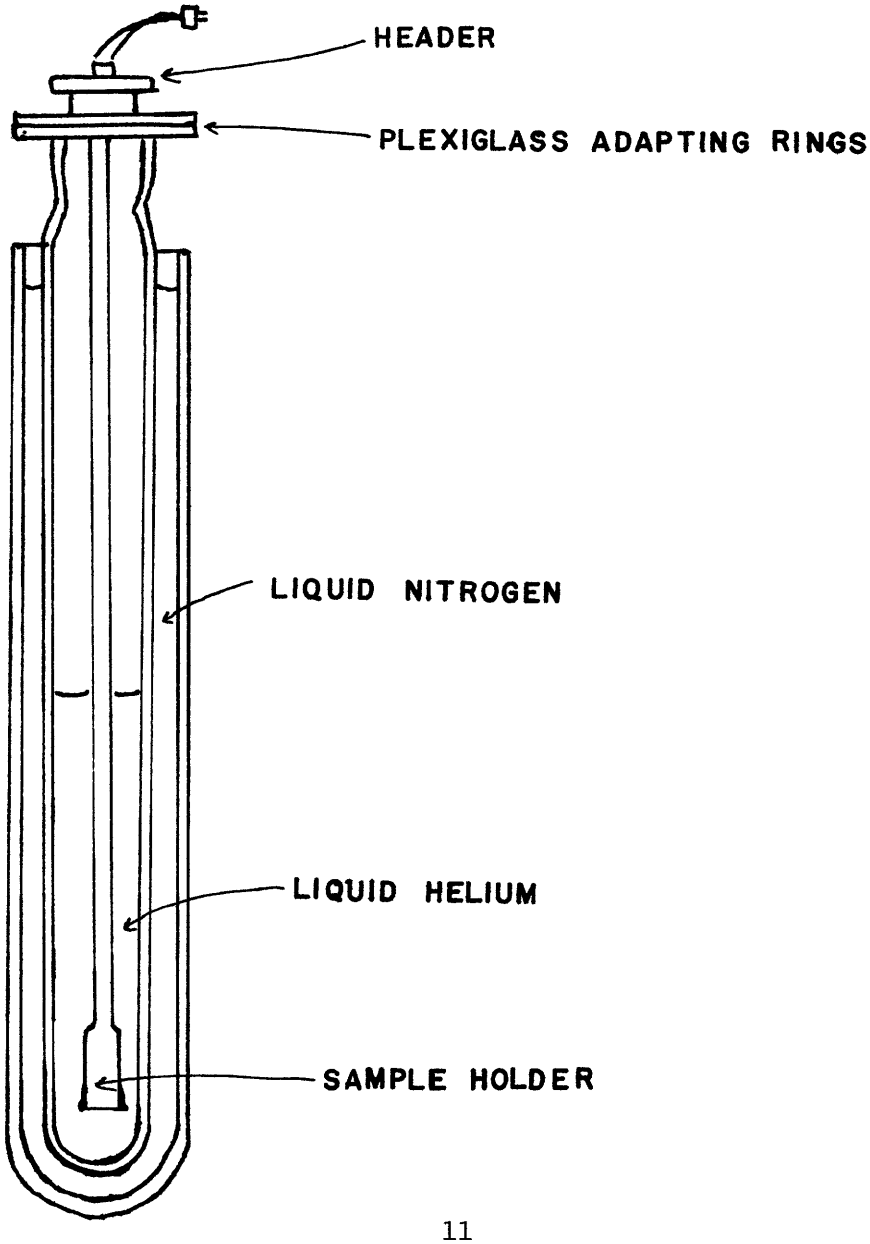
HEADER
PLEXIGLASS ADAPTING RINGS
LIQUID NITROGEN
LIQUID HELIUM
SAMPLE HOLDER

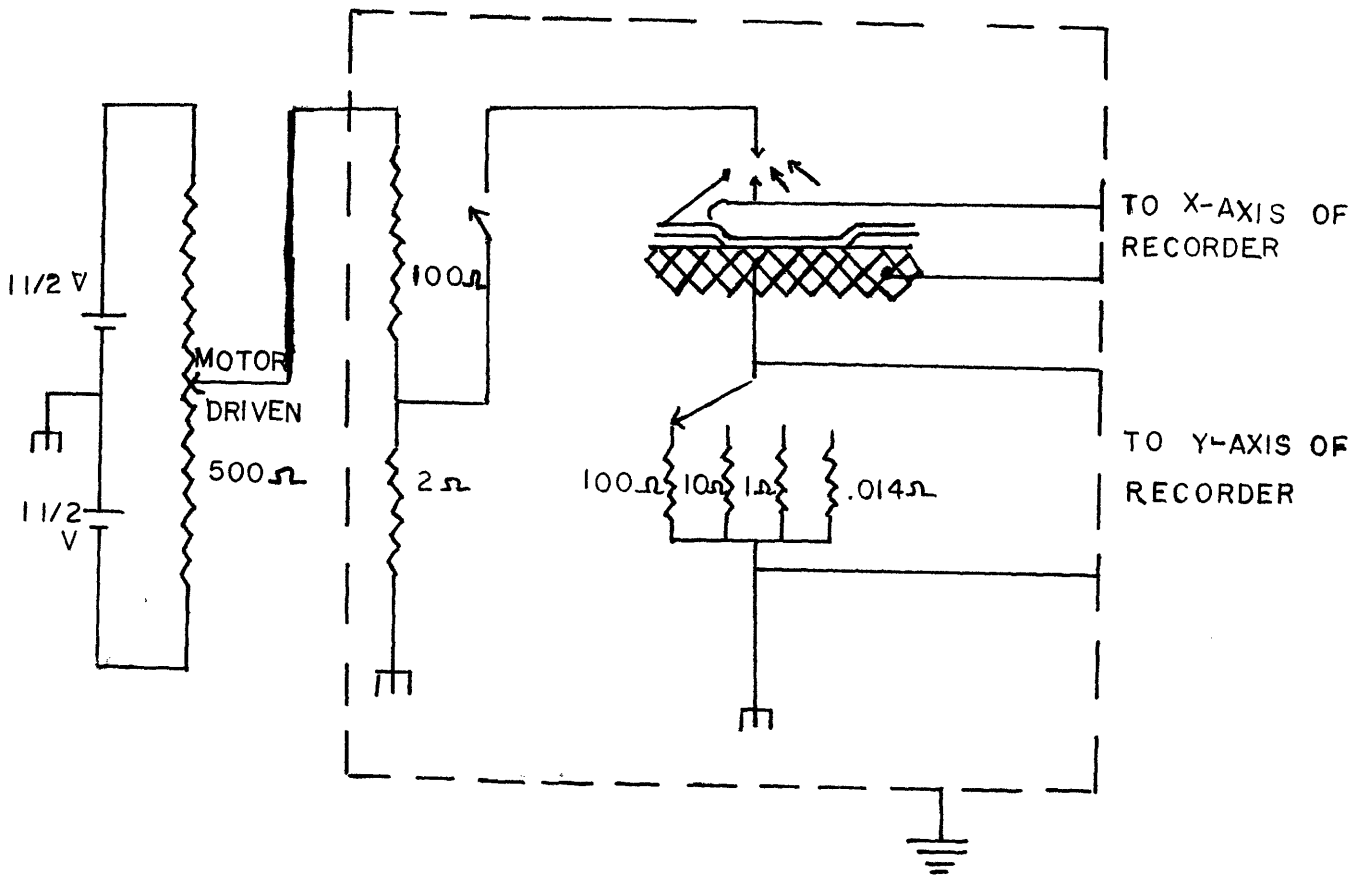

Tunneling Circuit

12

III. CONCLUSIONS

A. Experimental Results

Shown in Figures 13 through 20 are the I-V tunneling curves for junctions. In some instances, there is more than one curve shown for a particular junction; these are indicated. Given on the graphs are the oxidation times, oxidation temperatures, and testing temperatures for the junctions whose I-V curves are shown. As is obvious, there are no definite negative-resistance regions for any of the curves shown. However, it is possible to say a few things about the curves in Figures 14, 15, 19, and 20.

Looking at Figures 19 and 20 we notice very erratic behavior of the junction, especially near zero applied volts. This behavior could be attributed to the presence of shorts in the oxide barrier. This could be possible because the oxidation time for this junction was about half that for the other junctions. Also, there is the possibility of trapped water vapor in the oxide which could contribute to erratic behavior or reduce the gap value at the surface. But even with the erratic behavior, there is structure (sometimes faint) at 0.495 meV, 1.0 meV, 1.3 meV and 1.55 meV which could represent tunneling events. The structure at 0.495 meV could correspond to double particle tunneling as could the 1.55 meV structure. The very slight peak at 1.0 meV could represent a difference peak. The structure at 1.3 meV is unexplained. There is no apparent sum peak.

In analyzing the curves in Figures 14 and 15, there are two ways of approaching the problem. One is to assume that actual superconductor-insulator-superconductor tunneling is going on but the tunneling current

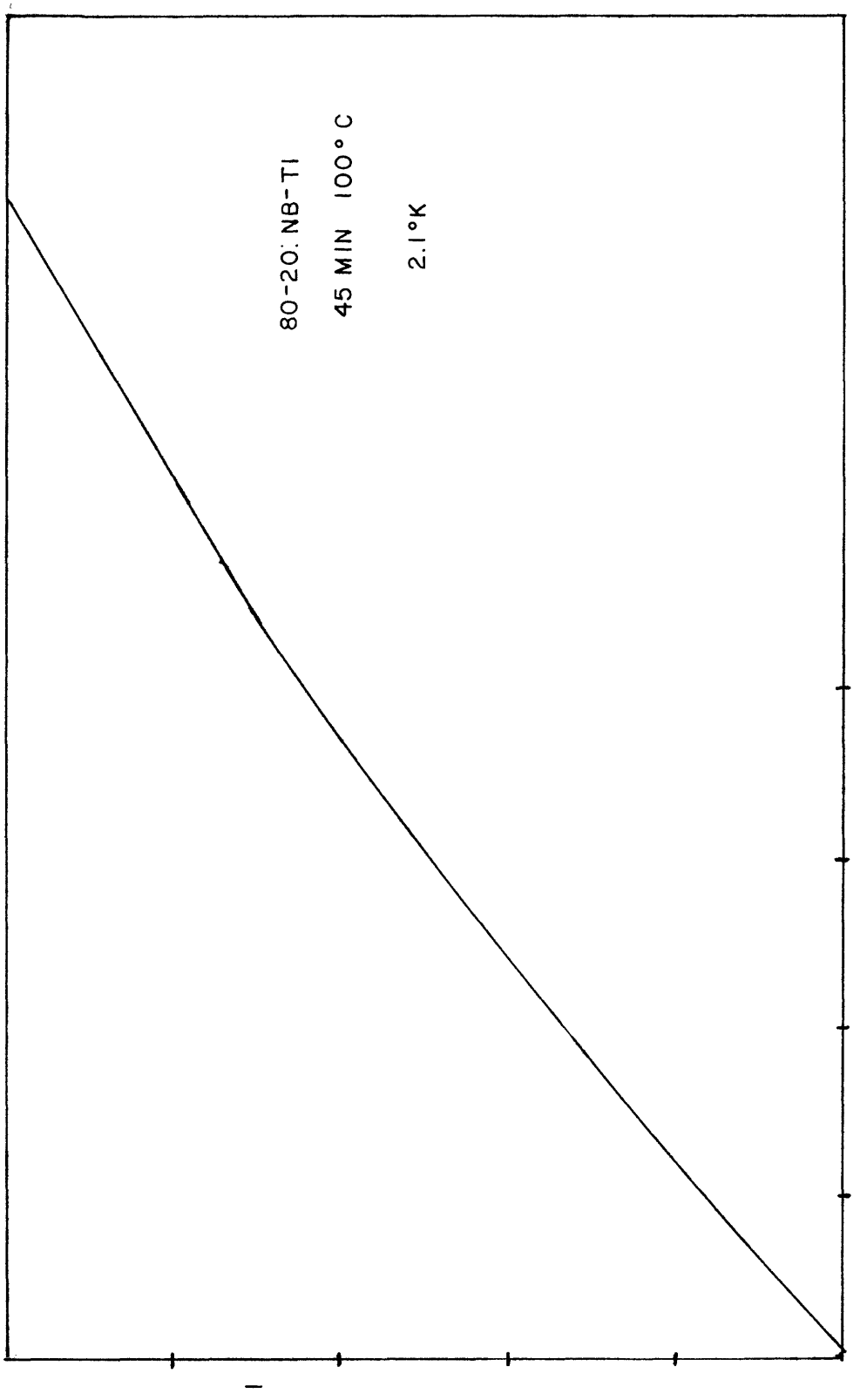

Graph 1
13

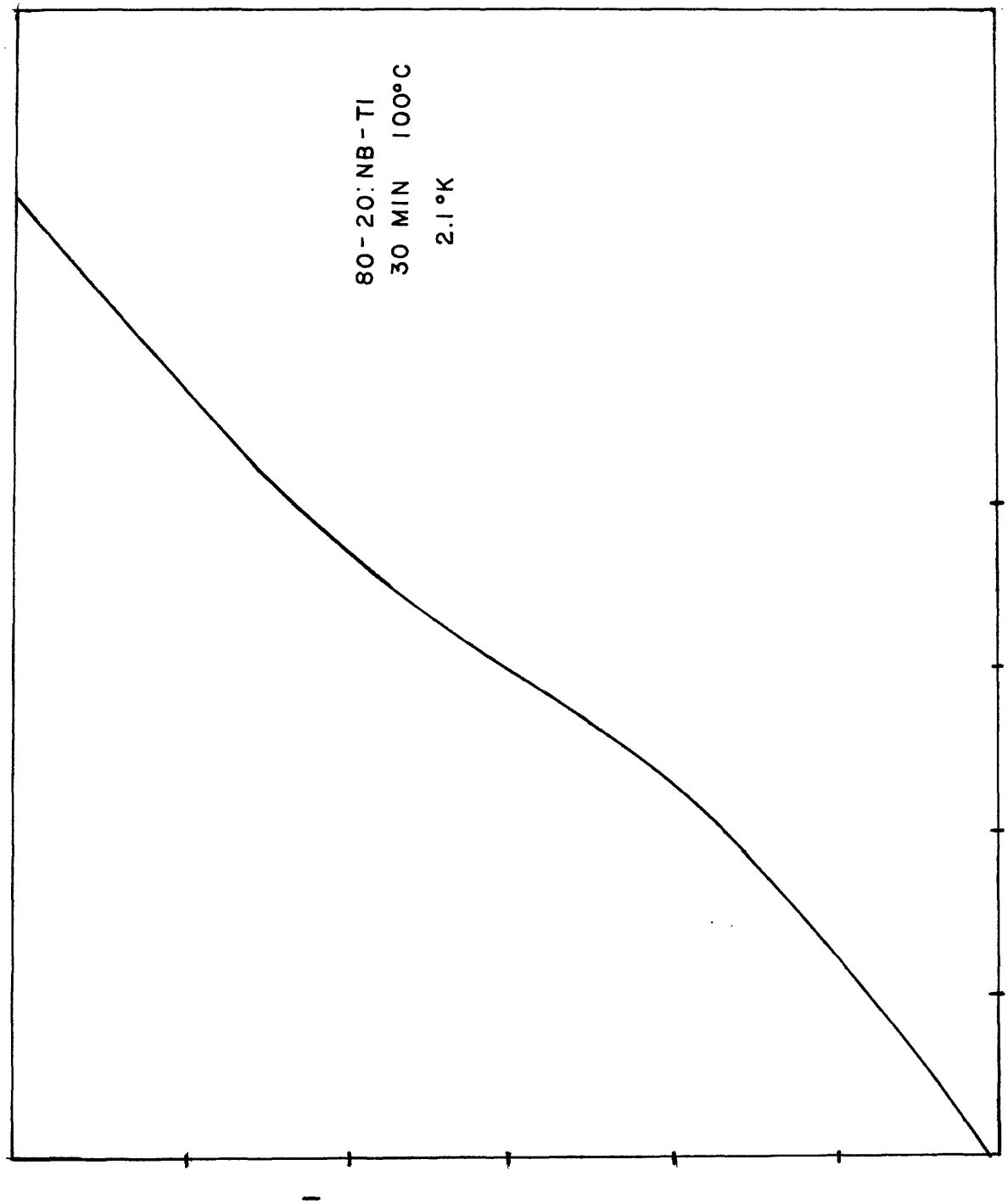

Graph 2a
14

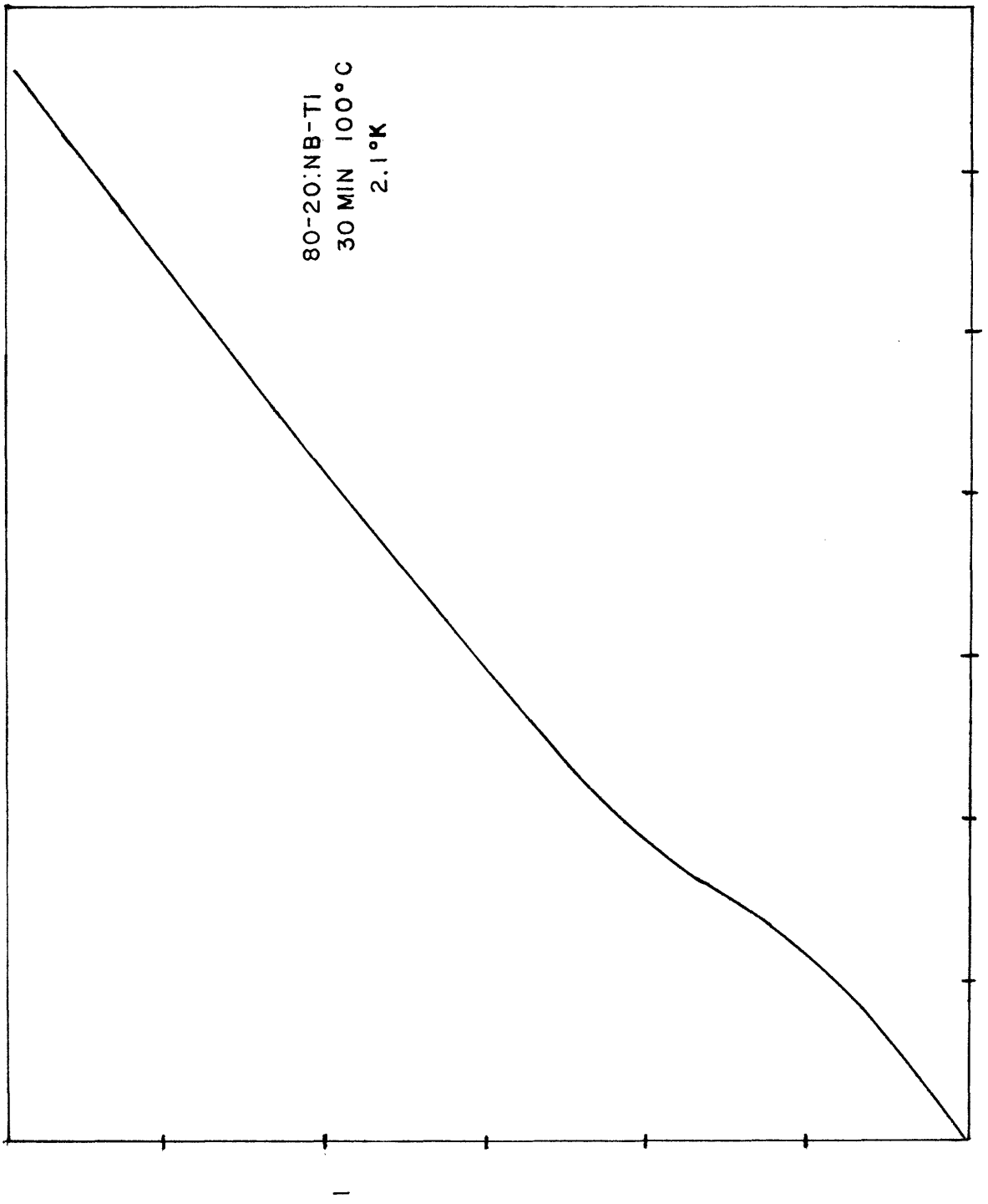

Graph 2B
15

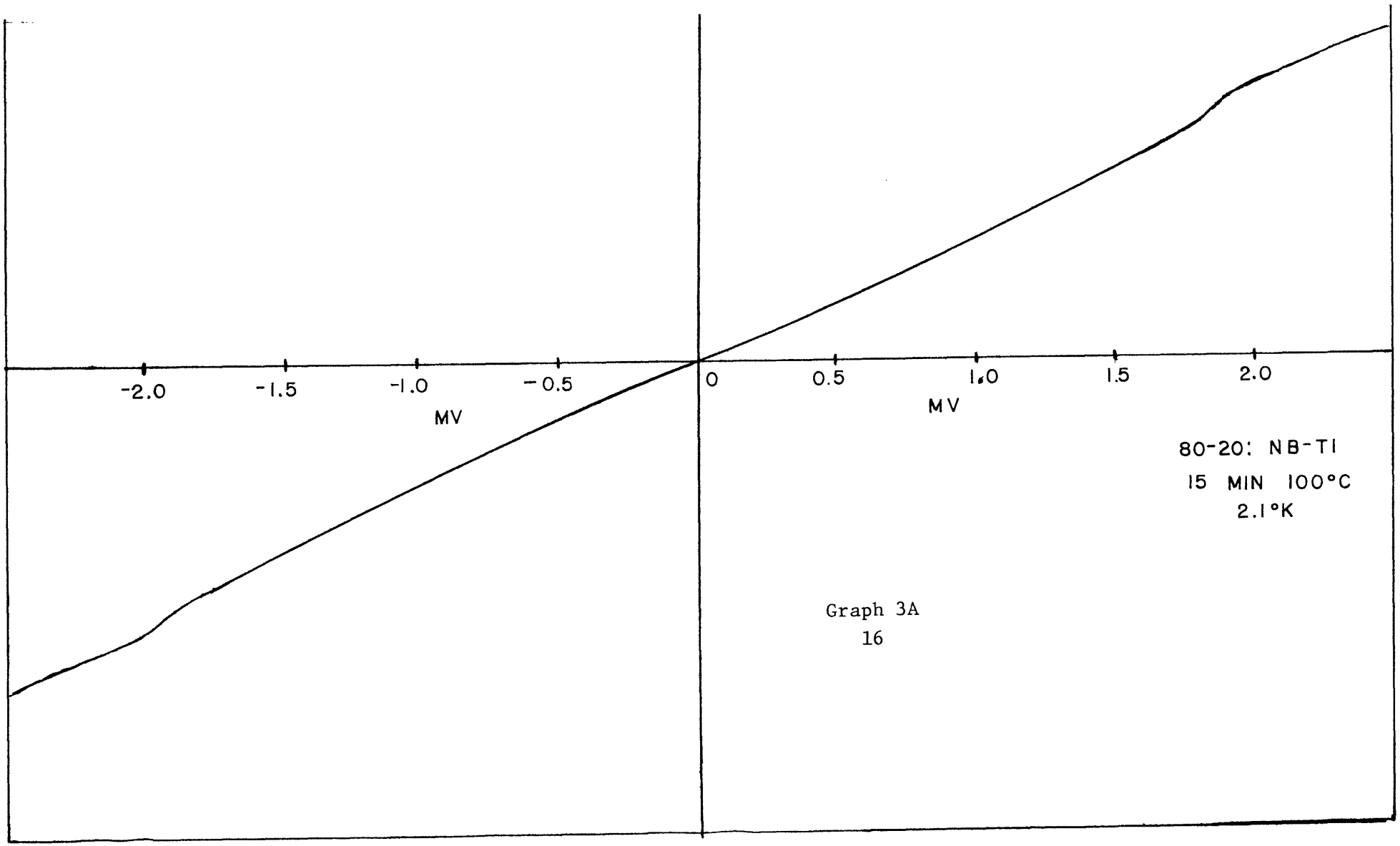

Graph 3A
16

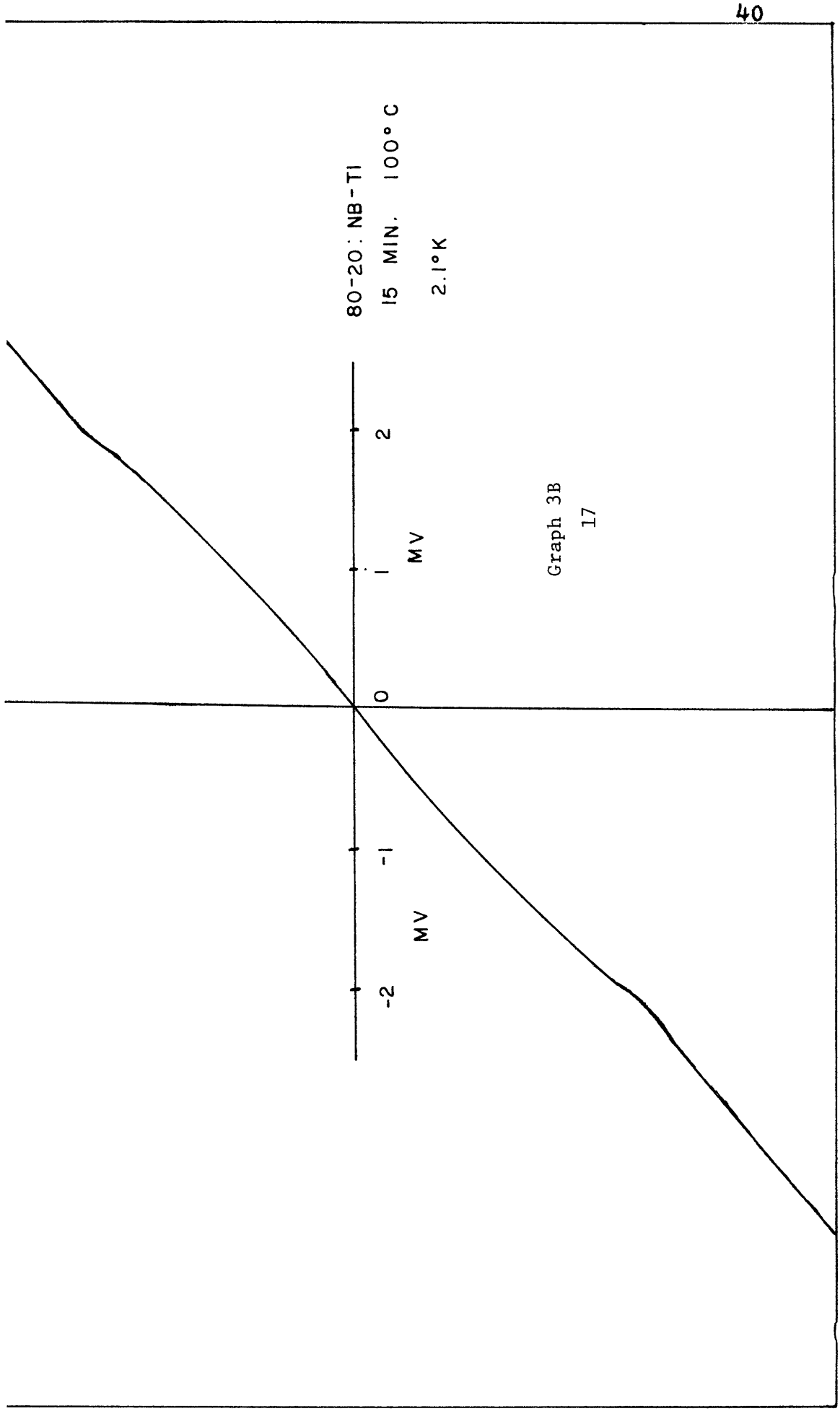

Graph 3B
17

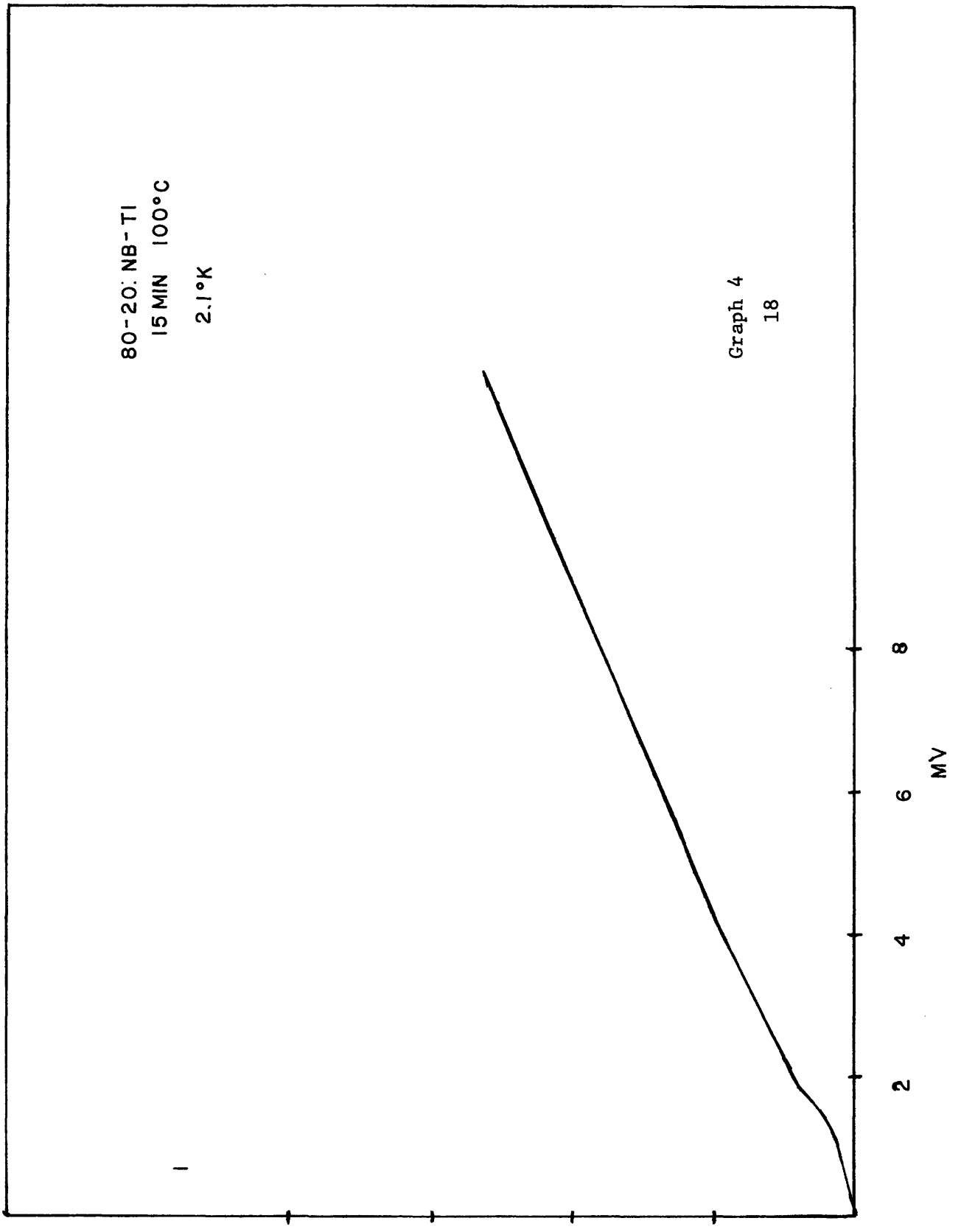
80-20: NB-Ti
15 MIN 100°C
2.1°K
Graph 4
18
2
4
6
8
MV

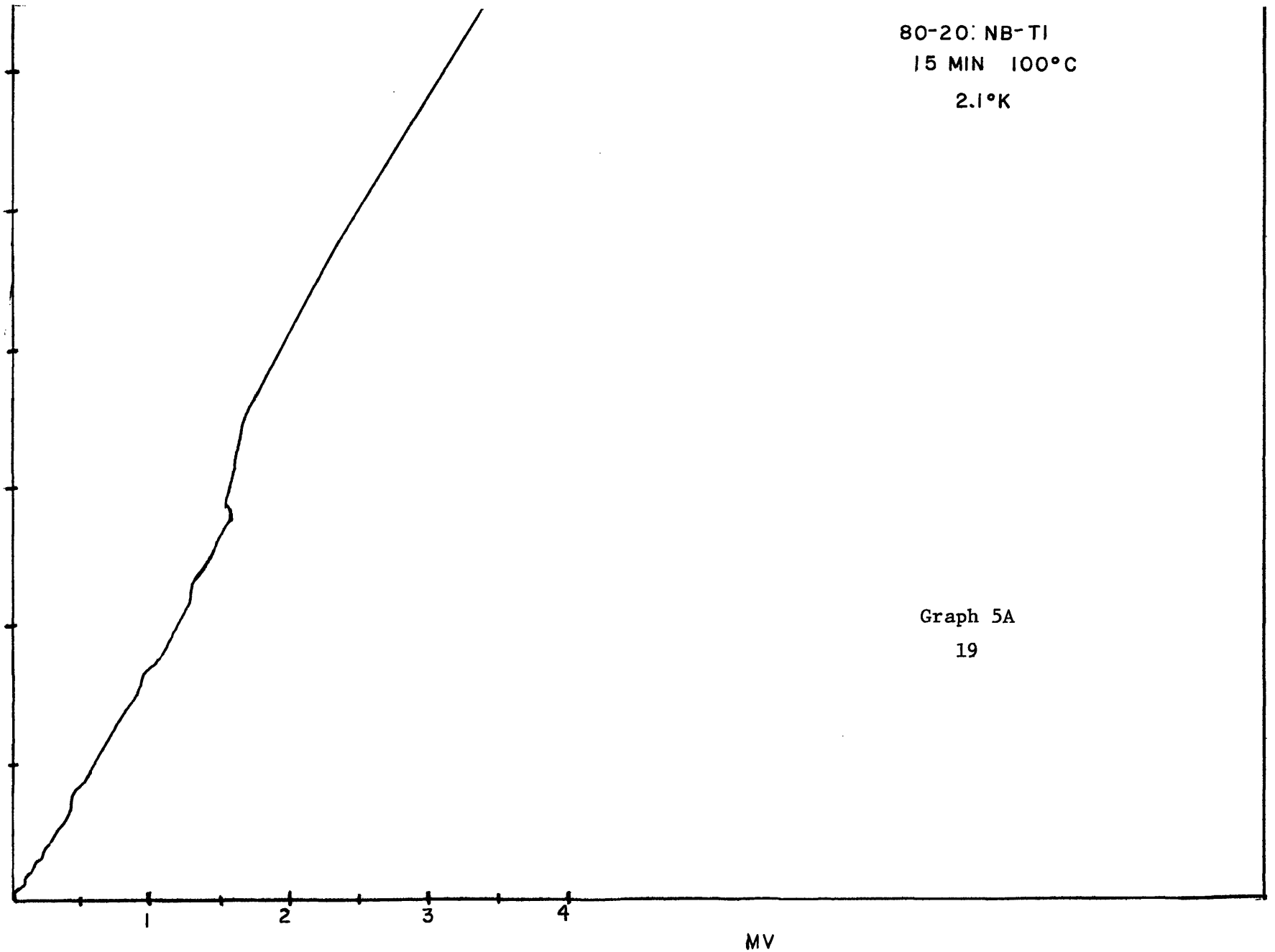

Graph 5A

19

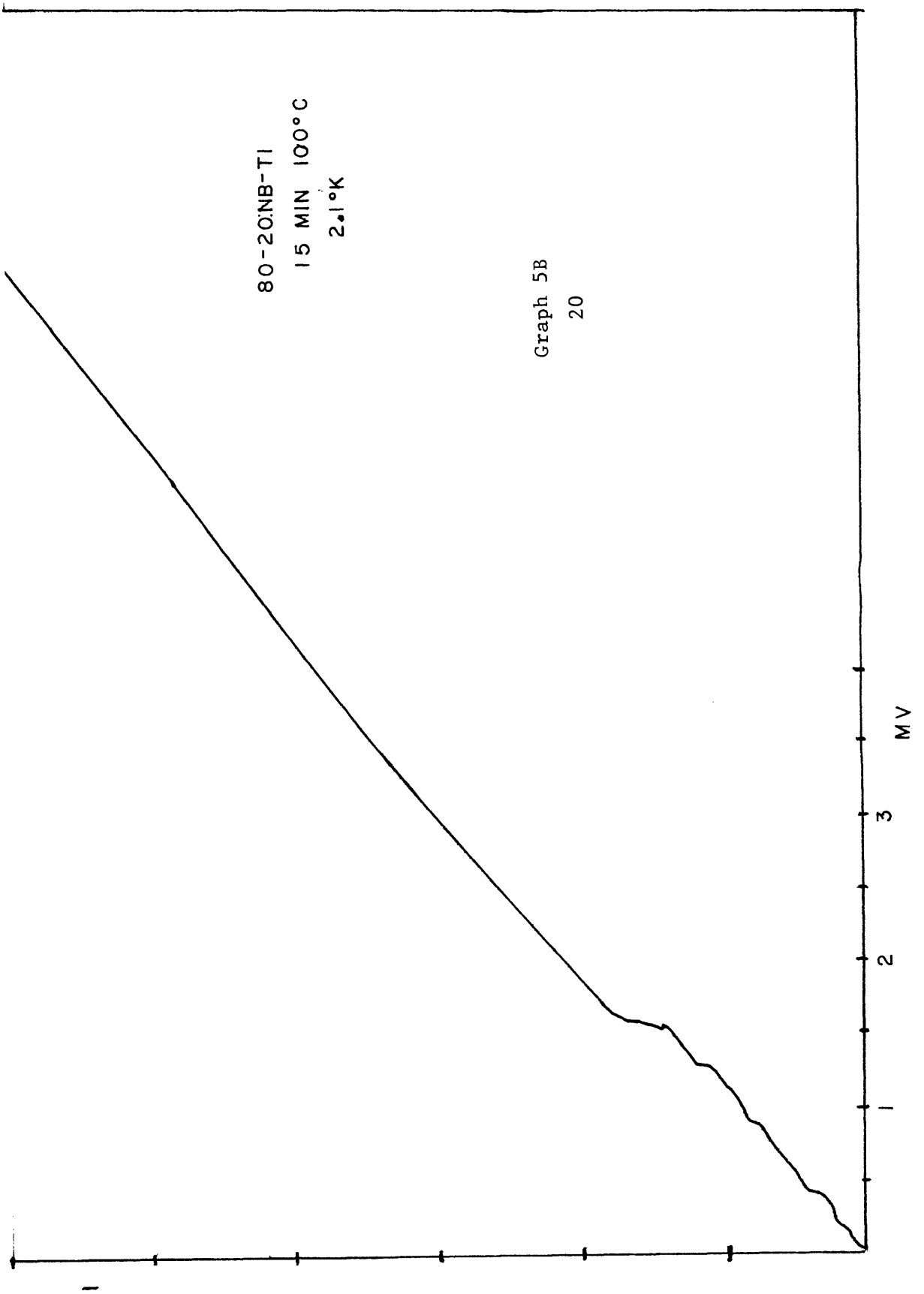
80-20 NB-Ti
15 MIN 100°C
2.1°K
Graph 5B
20
1
2
3
MV

is being damped out by oxide effects (to be explained below), and to assume further that either the temperature of testing was low enough to wipe out the difference peak (which could be the case considering tunneling done on niobium-niobium oxide-tin by Townsend and Sutton[25]), where reducing the temperature to 2.1°K practically wiped out the difference peak or the gap value of the niobium-titanium was reduced by oxide effects to a point where the difference peak would not appear. If this were the case, then using the schematic model of a tunneling curve discussed relative to Figure , then, effectively, the point (*) where $\frac{(dI/dV)_{supercooling}}{(dI/dV)_{normal}} = 1$, that is, the point of inflection just before the I-V characteristic becomes ohmic, would be a measure of the gap sum value. This is because the slope of the ideal curve beginning at $\varepsilon_1 + \varepsilon_2$ is practically straight up due to peaking in the density of states at gap edge. Looking at the curves, and evaluating as well as possible by mechanical measurements of slope changes, the point of inflection is at 1.85 meV. This value seems to be a possible gap sum value when compared with the predicted value (1.98). An alternate approach would be to assume that at the surface of the alloy the energy gap is reduced to zero and, therefore, according to the model discussed in connection with Figure 28, the point of inflection mentioned above would be a measure of the half-energy gap in Indium. In this instance the value of 1.85 meV which we obtain is certainly not near the expected half energy gap of Indium (.535 meV).

B. Discussion

The oxide effects mentioned above, which could attenuate the tunneling current and, therefore, give the curve the appearance it has, are the same ones discussed in the section dealing with such effects. The effect of oxide (and other contaminants) in reducing the gap value of the niobium-titanium alloy is the same effect (in the author's mind) which could make the surface of the alloy effectively normal. This effect is discussed quite extensively by Cohen, Cody and Goldstein[21] in connection with tunneling in Nb_3Sn. According to them, it is reasonable that only those particles within an electronic mean free path (ℓ) of the surface of a bulk superconductor contribute to the tunneling current. Thus, if the energy gap at the surface is reduced over a region approximately equal to ℓ, the effective gap observed in a tunneling experiment would be correspondingly small.

If we refer back to the mode of preparation of the specimens, we remember two things. One is that the mechanical polishing caused friction heating which was assumed to have produced local oxidation of the alloy. Secondly we recall that one of the purposes of annealing the specimens at temperatures around 1300°C was to hopefully break up a little of the oxide formed and cause the oxygen to diffuse into the surface of the alloy. Considering the great affinity of titanium for oxygen, it is reasonable to assume that much of the oxide coating on the alloy is some form of a titanium oxide. Considering this and considering the toughness of titanium oxides, it is highly unlikely that much of the oxide would be broken up by the anneal described above. Furthermore, if any of the oxide did break up and diffuse into the alloy, it probably would not diffuse in much more than

a few electronic mean path lengths. Consequently, this mode of preparation probably left the alloy with an oxygen-saturated surface, the oxygen content being enough to suppress or diminish superconductivity in this region. What would be left then would be either a superconductor with a drastically reduced energy gap (hence probably no negative resistance region), or effectively a normal metal (hence tunneling behavior such as that between a normal metal and a superconductor). Since the normal metal-superconductor proposition is not borne out by observed inflection point values , then the idea of a superconductor with a reduced gap seems plausible.

The specimen, prepared by the electropolishing method mentioned above, was tested and displayed very erratic behavior and in fact gave no tunneling curve whatever. This junction behavior was attributed to adsorbed contaminants from the electrolyte and to trapped water vapor and hydrogen gotten from the immersion of the specimen in the hydrogen peroxide solution. The peroxide solution which was designed to oxidize the specimen was probably so dilute that whatever oxide was formed was perforated by trapped water molecules.

C. Suggestions for Further Research

In considering the difficulties mentioned above, two techniques for fabricating junctions come to mind. One is the following: to electropolish the specimens as described previously. This would eliminate mechanical polishing difficulties. Now if this polished specimen were given a high temperature anneal in high vacuum, most adsorbed impurities and

trapped water molecules would be driven off, leaving the surface of the specimen relatively free of contanmiants. The specimen would now be put into a heated oxygen atmosphere, similar to that described previously, to form a thermally grown oxide coating. This method of fabricating an oxide barrier seems successful in light of the absence of erratic behavior in the junctions which were oxidized for at least thirty minutes in heated oxygen. The second method would be to electropolish a specimen, anneal it in high vacuum, and then to oxidize it by submitting it to a glow discharge in oxygen. This procedure would be analagous to the anodization procedure described by Miles and Smith,[22] Jennings, McNeill and Solomon,[23] and Tibol and Hull.[24] This anodization would normally take place in a gaseous oxygen atmosphere of about fifty microns pressure. This procedure has two advantages. One is that the sample could be oxidized without exposure to air after the anneal. The other is that dry oxygen can be used in the glow discharge by introducing pure oxygen into the system through a drying calcium hydride tube. This would eliminate further difficulties with trapped water molecules. The author feels that these two suggested methods of fabrication are very worthy of investigation since they eliminate difficulties associated with previous techniques of preparation without introducing any apparent further difficulties.

REFERENCES

1. H. Kamerlingh Onnes, Akad. Van Weten schappen (Amsterdam) 14, 113, 818 (1911).

2. F. London, Proceedings of the Royal Society, A152 24 (1935).

3. V. L. Ginzburg, Zhur. Eksp. Teor. Fiz. SSSR, 14, 134 (1946).

4. E. Maxwell, Phys. Rev., 78, 477 (1950).

5. L. H. Cooper, Phys. Rev., 104, 1189 (1956).

6. J. Berdeen, L. N. Cooper, J. D. Schrieffer, Phys. Rev., 106, 162 (1957); 108, 1175 (1957).

7. M. Tinkham, Superconductivity, Gordon and Breach Pub., New York, 1965.

8. J. Bardeen, Phys. Rev. Lett., 6, 57 (1961).

9. B. N. Taylor and E. Burstein, Phys. Rev. Lett., 10, 14 (1963).

10. J. R. Schrieffer and J. W. Wilkins, Phys. Rev. Lett., 10, 17 (1963).

11. B. D. Josephson, Phys. Lett., 1, 251 (1962).

12. S. Eisberg, Fundamentals of Modern Physics, J. Wiley & Sons, N. Y., 1961.

13. I. Giaever and K. Megerle, Phys. Rev., 122, 1101 (1961).

14. M. L. A. MacVicar, Sc.D. Thesis, Department of Metallurgy and Materials Science (1967).

15. G. Goetz, private communication.

16. B. T. Matthias, Progr. Low. Temp. Phys. 2, 138. I, 10; X, 3.

17. R. D. Blaugher and J. K. Hulm, J. Phys. Chem. Solids, 19, 134 (1963) X, 3.

18. R. D. Blaugher, B. S. Chandrasekhar, J. K. Hulm, E. Corenzwit and B. T. Matthias, J. Phys. Chem. Solids, 21, 252 (1961) X, 3.

19. D. H. Parkinson, Reports on Progress in Physics, Vol. XXL, The Physical Society, London (1958).

20. John M. Blatt, Theory of Superconductivity, p. 358 (1964) Academic Press, Inc., New York, New York.

21. R. W. Cohen, G. D. Cody and Y. Goldstein, RCA Review, Vol. XXV, 510 (1964).

22. J. L. Miles and P. H. Smith, J. Electrochem. Society, 110, 1240 (1963).

23. T. A. Jennings, W. McNeill, R. E. Solomon, J. Electrochem. Society, 110, 1240 (1963).

24. George J. Tibol and Robert W. Hull, J. Electrochem. Society, 111, 1368 (1964).

25. P. Townsend and J. Sutton, Phys. Rev. 128, 591 (1962).